

BROKEN SYMMETRY AND COHERENCE OF MOLECULAR VIBRATIONS IN TUNNEL TRANSITIONS

Alexander M.Dykhne^{1,2}

¹*TRINITI, 142092 Troitsk, Russia*

Alexander G.Rudavets²

²*Moscow Institute of Physics and Technology, 141700 Dolgoprudny, Russia*
Arudavets@mics.msu.su*

Abstract We examine the Breit-Wigner resonances that ensue from field effects in molecular single electron transistors (SETs). The adiabatic dynamics of a quantum dot elastically attached to electrodes are treated in the Born-Oppenheimer approach. The relation between thermal and shot noise induced by the source-drain voltage V_{bias} is found when the SET operates in a regime tending to thermodynamic equilibrium far from resonance. The equilibration of electron-phonon subsystems produces broadening and doublet splitting of transparency resonances helping to explain a negative differential resistance (NDR) of current versus voltage (I-V) curves. Mismatch between the electron and phonon temperatures brings out the bouncing-ball mode in the crossover regime close to the internal vibrations mode. The shuttle mechanism occurs at a threshold V_{bias} of the order of the Coulomb energy U_c . An accumulation of charge is followed by the Coulomb blockade and broken symmetry of a single or double well potential. The Landau bifurcation cures the shuttling instability and the resonance levels of the quantum dot become split because of molecular tunneling. We calculate the tunnel gaps of conductivity and propose a tunneling optical trap (TOT) for quantum dot isolation permitting coherent molecular tunneling by virtue of Josephson oscillations in a charged Bose gas. We discuss experimental conditions when the above theory can be tested.

Keywords: Nanoelectromechanics, Coulomb blockade, broken symmetry bonding, electro-optical traps

*address for correspondences

*This paper is dedicated to the
blessed memory of
A.P.Kazantsev*

1. Introduction

In this new millennium, we are witnessing the birth of molecular electronics, which can now operate with a single atom or a molecular nano-scale cluster called a quantum dot. Each quantum state of the dot can be characterized by electron tunneling, since the position of its discrete level is not averaged due to thermal spreading $k_B T$, especially at cryogenic temperatures T such that $\Delta E \gg k_B T$, where the ΔE is the energy spacing between levels and k_B denotes the Boltzmann constant. The quantum dot is confined between electrodes in a composite nano-scale system. Typically, the molecular cluster is trapped on the surface of a lead by a Lennard-Jones or van der Waals like potential. The electronic reservoirs are set out of equilibrium by applying a bias voltage V_{bias} , which modifies the electrochemical potentials (Fermi levels) of each electrode μ_σ driving a current through the quantum dot. The question arises: What kind of the coherent properties one would expect by measuring the electron transport in such system?

The experiments with nanoclusters, e.g. including fullerene molecules C_{60} [1] and C_{140} [2], which were addressed in a single electron transistor (SET), reveal a plethora of new behavior, which cannot be explained within the framework of solid-state nanostructures [3] theory. For instance, there are rich structures of conductivity resonance in a magnetic field [4] and anomalously high Kondo temperatures, above $50K$, found in [5]. The conductivity gap is well correlated with the resonant frequency $\Omega = 5$ meV of the "bouncing-ball" mode of C_{60} and manifests itself as an enhancement of the conductance. There are two schools of thought, which attribute this enhancement either to Frank-Condon transitions or to the shuttling instability [7] - [14] discussed below. For both schools the issue of quantum mechanical coherence is the matter of a considerable concern. We reconcile the above points of view in the adiabatic approximation, i.e. by assuming that electronic degrees of freedom are much faster than that of the dot. This is the case of local equilibrium in phase space between the electronic flows and the dot dynamics. Can the electron flow dephase the quantum dot by scattering off it?

From first sight, there is a physical constraint for dephasing, since an electron passing through the dot carries information in one direction, which is fixed by the bias voltage. This produces an asymmetry (chirality mapping) that accompanies the charging, by virtue of the electron affinity to the quantum dot. The charging modifies the Coulomb energy that competes with the elastic deformation potential of the dot. Thence, the Coulomb potential breaks the orig-

inal symmetry of the molecular bonds in such a way that the growth of V_{bias} produces a bifurcation of the bonding potential. The broken symmetry signifies the existence of a border for the non-demolition quantum measurements. The quantum-classical transition can thus be detected by the broken phase of the oscillating current.

We have seen that the phase coherence of the oscillating current is affected by the tunnel coupling to thermal reservoirs due to the itinerant electrons. The phase-breaking process also changes the interface states as a result of interaction with other electrons via global Coulomb blockade. The Coulomb energy of electrons and holes forces their coherent reorganization. The electron coherence length L_e increases with decreasing temperature $k_B T$. As a result of freezing, $k_B T \leq 1$ mK, a solid-state system becomes mesoscopic on scales $L_e \leq 1 \mu m$.¹ Under this condition, the description of transport in terms of the local conductivity breaks down. The transport in a ballistic regime is dominated by electron scattering from the interface but not from the quantum dots. Most investigations of nanoscale systems are carried out for ballistic dots, whose theory and experiment have together formed a new realm of mesoscopic physics [3]. For instance, observation of the Kondo effect in single-atom and single-molecular junctions has led to a promising field called spintronics [15].

The SET device reported in [1] is an example of a double tunnel junction system in which the quantum dot self-oscillates between the leads. The mode softness significantly influences the electronic transport due to the effect of mechanical deformation on the electrical properties. Nanoelectromechanics (NEM) ensures that the electron's phase can be preserved over distances larger than the dot size, thus giving rise to a quantum interference which cannot be observed in macroscopic conductors. The conductance of dots could inherit this quantum coherence, which can manifest itself in superconducting current echoes [6], for instance. It means that a single molecular NEM-SET could, in principle, display a high charge sensitivity, enabling non-demolition measurements at the quantum threshold.

The experiments going under this title encompass a wide range of the electro-mechanical devices from the macro- to nano-scale. Coupling of a mechanical oscillator to non-equilibrium baths is accompanied by stiff dynamics of elastic self excitations and brings the charge transfer into the shuttle regime as a result. The evident advantage of shuttling lays in avoiding the tunnel coupling bottleneck. The phenomenon of the shuttle instability for quantum dots in double junctions resembles a more general class of the adiabatic quantum pump for electroacoustic and/or photovoltaic effects [11].

¹When the electron's phase coherence length L_e , i.e. the typical distance for the electron to travel without losing its phase, is of the order of the dot mean free path L_d , such a system is called mesoscopic. The regime ensuring $L_e \gg L_d$ is called ballistic.

The current control at the one-by-one electron accuracy level is feasible in mesoscopic devices due to quantum interference. Though the electric charge is quantized in units of e , the current is not quantized, but behaves as a continuous fluid according to the jellium electron model of metals. The prediction of the current quantization dates back to 1983 when D. Thouless [16] found a direct current induced by slowly-traveling periodic potential in a 1D gas model of non-interacting electrons. The adiabatic current is the charge pumped per period, I , and has to be multiple of the electron charge, i.e. $I = e\nu N$, where the frequency $\nu = V/A$ is related to the traveling wave velocity V and the wavelength A . Then the charge transmitted in the adiabatic pump is period-independent.

The frequency dependence of the current I holds true for a dot shuttling between the leads and thereby modulating in phase the conductivity of the sequential tunnel junctions. The electron interference is manifested in an instability of the dot charge, which is subject to either stochastic or periodic oscillations. These shuttle dynamics allow one to find a new compromise between tunnel charging and Coulomb forces, rigidity and elasticity of dot bonds. Yet, a simple scattering theory that would help to estimate a measurements of current induced by the shuttling is absent, to our knowledge. Even for the usual I-V curve, characterized by regions of negative differential resistance and observed experimentally in [1], a mutual consensus between the Franck - Condon picture of electron transport and the shuttling mechanism has not been found.

In the quest for a new functionality of NEM SET, the shuttling mechanism has attracted a considerable interest as an effective method of control of electron transport, whose current depends on the frequency ν . A description of the shuttling instability can be based on a general master equation [7] and Green's function [14] methods of coarse grained dynamics over a scattering spectrum, without paying special attention to resonance field effects. Almost all of the obtained results are strongly model dependent and do not shed light on the underlying physics. For example, remaining unexplained are the higher Fano factors in the shuttling regime as compared to that obtained in the tunneling regime[17]. This is one reason why it is worthwhile to develop a conceptually clear picture of the phenomenon, in the spirit of the Breit-Wigner theory of resonance cross sections. Another reason for this is that many results obtained both in the framework of the scattering approach and by classical methods in mesoscopic physics are applicable on an equal footing to the shuttling process [18].

The universality of both the Breit-Wigner method [18] [19] and the shuttling is manifested by studies of the NEM Josephson junctions [7], [22]. The latter belong to the mesoscopic system wherein the Cooper-pair box is shuttled between remote electrodes in the superconducting SET (SSET). The NEMs favor coherent coupling[22] and allow the suppression of quantum fluctuations

of dissipationless persistent current in the ground state of the system. The shuttle mechanism reduces the Fano factor at low temperatures of about 1 mK [7]. This is in accordance with the general rule [18] that the voltage, the current, and the charge oscillations due to Josephson plasmons are less noisy and more entangled for strongly correlated system.

The shuttle mechanism based on the tunnel Hamiltonian[7]- [14] is equivalent to the simplest possible Holstein-type polaron models ². These models ignore all complexity of the real molecular SETs: A detailed understanding of the charge screening, geometry of electrodes, hybridization with continuous and bound surface states, scattering off impurities is either absent or presented in a fragmented manner. The lack of knowledge about frequency shifts of the scattering resonances is filled by a phenomenological approach. Taking for granted their argumentation, we tackle the tunnel resonances using a common theory of resonance scattering in the Breit-Wigner approximation with a more pragmatic goal. By developing the Born-Oppenheimer adiabatic strategy in forbidden (for electrons) inter-electrode zone, where quantum dots are allowed to move classically, we present here the current and the quantum-dot charge in a self-consistent, model independent, and tractable form.

In Sec. 2, we discuss the Landauer formula for the current, deriving it in parallel with inferring the mean charge from detailed balance conditions. This is followed by deducing the resonant tunneling in the Breit-Wigner approximation, which provides a convenient framework for description of quantum transport phenomena. In Sec. 3, the dissipative tunneling is taken into account with the help of a phenomenological model. In Sec. 4 we make use of adiabatic dot dynamics in order to describe field splitting and broadening of the resonance levels. The main aim is to show how do the dot oscillations between the leads influence markedly the current-voltage curves. With an increasing voltage the charging regimes change. Section 5 is dedicated to the Coulomb blockade modified by the adiabatic motion in phase space. We calculate the self-consistent charge accumulated in resonance windows of conductivity in order to illustrate the tunnel term transformation from a single well symmetry to a double well symmetry. We analyze how the shuttling instability depends on bias voltage. In Sec. 6 we estimate the shot noise of the shuttling adopting the resonance scattering approach. In Sec. 7 we justify the assumption of broken symmetry of the tunnel terms by employing a quantum treatment of the SET setup in the Born-Oppenheimer adiabatic approach. In Sec. 8 we propose the use of TOT protection of a quantum dot from parasite hybridization with the substrate surface in order to avoid dissipative tunneling roadblocks.

²the coupling of Einstein phonons to finite electron density in conduction band.

Coherence of electron transport via double wells is sketched briefly in Sec. 9. Conclusions are given in Sec. 10.

2. The Landauer formula.

The Landauer's seminal suggestion, that the current is transmission, dominates in mesoscopic physics and has applications to a variety of systems, including the electron transport in solids, liquids, quantum wires and dots. First and foremost, this theory describes conductance by purely dissipationless electrons scattering. Pursuing the NEM phenomena, we shall follow a similar reasoning, omitting the non-elastic effects on the microscopic scales.

Consider a ballistic quantum dot between two metallic terminals. Their electronic reservoirs are held at the thermal equilibrium described by the Fermi-Dirac distribution

$$f_\sigma(E) = \frac{1}{1 + e^{(E - \mu_\sigma)/k_B T}}, \quad (1)$$

where the chemical potentials $\mu_{l(r)} = E_F \pm eV/2$ correspond to a shifted Fermi energy, E_F , while eV is the biased electron potential across the source and drain leads. Electrons flow from the high potential μ_l to the low potential μ_r passing the Fermi level E_F . The electronic scattering state ψ with the Fermi energy E is normalized to unit flux in the lead $\sigma \in (l, r)$ at far asymptotic distances $\chi = \pm\infty$ from the quantum dot placed at a fixed coordinate x . The partial current of electrons, averaged over the momenta $p(E) = \sqrt{2mE}$, where m is electron mass, is defined as

$$I_\sigma(\chi, t) = \frac{e}{m} \text{Im} \int_0^\infty \frac{dp(E)}{2\pi} \psi_\sigma^*(\chi, t) \frac{d\psi_\sigma(\chi, t)}{d\chi} f_\sigma(E). \quad (2)$$

The measured current from the source to the drain electrode is proportional to the energy integral of squared modulus of the scattering matrix $|S(E)|^2$, whose integrand is called the quantum-dot transparency

$$\Upsilon(E) = |S(E)|^2,$$

overlapped with the difference of Fermi functions of the electrons in the right and the left leads

$$I = I_r(\chi = \infty, t) + I_l(\chi = -\infty, t) = \frac{\pi e}{\hbar} \int_0^\infty dE \Upsilon(E) (f_r(E) - f_l(E)). \quad (3)$$

Here \hbar is Plank's constant. The only quantum property playing a role in the average current I is the Pauli principle, which dictates that each quantum state in the Fermi sea has to be occupied by a single electron. This means that only

a fixed number of electrons can be accumulated in the scattering sector at a fixed energy E , thus setting a limit on the average current flow I . Factor 2 in Eq. 3, representing the electron spin degeneracy, has to be carefully taken into account, especially for the detailed balance conditions, as demonstrated in Sec. 3 and used in Sec. 5. At small bias, that is at $V \ll k_B T$, one writes $I = GV$, by introducing the linear conductivity G defined as

$$G = \frac{2e^2}{h} \int_0^\infty dE |S(E)|^2 \frac{df(E)}{dE}. \quad (4)$$

The Fermi-Dirac distribution, $f(E)$, is the step-like function of energy E , while its derivatives are delta functions in energy. One therefore obtains

$$G = g_0 |S(E_F)|^2.$$

The conductance quantum $g_0 = \frac{2e^2}{h}$ is a universal factor of maximum conductivity for a single scattering channel at unit transmission. The minimum quantum resistance is the inverse quantity $g_0^{-1} = 12.9 K\Omega$, which implies that the dissipation of an ideally transparent quantum dot occurs due to the scattering at the interface with electronic thermal reservoirs. This means that even for the system in a perfectly ballistic condition, the coupling of the electron with the reservoir induces decoherence. Irreversibility of an open system arises from uncorrelated "itinerant" electrons broadening the resonant state. "Itineracy" destroys the unitarity of the quantum mechanical evolution, and the scattering matrix S in the Landauer theory is reduced to phenomenological determination. Below, we present the Breit-Wigner resonance approximation for the scattering matrix as an example of such an approach.

Resonant tunneling in Breit-Wigner approximation. Let us consider the tunnel resistance of a $\chi = 1$ nm-broad vacuum gap between two gold electrodes. For the Fermi energy $E_F \sim 8eV$ and the work function $W \sim 5eV$, the dominating electron wave function exponentially decreases in vacuum with the rate $\gamma = \sqrt{2Wm}/\hbar \sim 1.3\text{\AA}^{-1}$, where m is the electron mass. The enormous resistance $R_{1nm} = g_0^{-1} e^{-2\chi\gamma} \sim 2.5 \cdot 10^{15}$ Ohm prohibits electron transport in vacuum in the absence of a quantum dot.

For a dot fixed between two electrodes, a weak electron coupling results from the tunnel current passing through the dot and broadens the resonant dot levels. The broadening width exponentially decreases as function of the distance χ between the dot and the electrode surface. The typical tunnel probability for an electron to jump from the electrode to the quantum dot formed by a C_{60} molecule [1] placed at the distance $\chi \approx 6\text{\AA}$ from the lead, can be estimated as $\Gamma_0 \sim E_F e^{-2\chi\gamma} \sim 0.1 - 1\mu eV$. In the situation when the quantum dot can move, its hybridization with the lead depends on the dot coordinate

$$\chi = \pm x$$

$$\Gamma(\chi) = \Gamma_0 e^{-2\gamma x}. \quad (5)$$

The dot is characterized by the two parameters $\Gamma^r = \Gamma_0 e^{2\gamma x}$ and $\Gamma^l = \Gamma_0 e^{-2\gamma x}$ describing the exponentially decreasing couplings $\Gamma^{l,r}$ with the reservoirs l or r . The total broadening $\Gamma = (\Gamma^r + \Gamma^l)/2$ denotes the width of the energy level E_{dot} . The broadening Γ may vary with the level energy and depends on the electron-electron correlation, although not strongly. In the weak-coupling limit, the resonance width Γ is much smaller than the average spacing between the energy levels Δ , $\Delta \gg \Gamma$. In this limit only the scattering energies E which are nearest neighbours to the dot energy level E_{dot} contribute to conductance. In this case, the Breit-Wigner resonance of the scattering matrix $|S(E)|^2$ or the transparency $\Upsilon(E)$ reads

$$\Upsilon(E) = |S(E)|^2 = \frac{\Gamma^r \Gamma^l}{(E - E_{dot})^2 + \Gamma^2}. \quad (6)$$

The scattering matrix elements implicitly depend on x via the parametric coordinate dependence of E_{dot} and Γ . The tunnel coupling Γ homogeneously broadens the resonance energy levels E_{dot} . Therefore, the Lorentzian distribution of the scattering matrix element implies an exponential decay via the coupling of electrons to the environment across only a resonance window of density of states $\rho(E)$

$$\rho(E) = \frac{1}{\pi} \frac{\Gamma}{(E - E_{dot})^2 + \Gamma^2}. \quad (7)$$

By substituting the matrix $S(E)$ from 6 into Landauer's formula 3 at zero-temperature limit, the tunneling conductance is exactly represented as

$$G_L(E_F) = g_0 \frac{\Gamma^r \Gamma^l}{(E_F - E_{dot})^2 + \Gamma^2}. \quad (8)$$

For the most of the experiments of interest, the temperature kT_B typically exceeds the resonance width $\Gamma \ll kT_B \ll \Delta$, and hence the interference effect of adjacent levels separated by the Δ is inessential. The conductance G from 4 is given by the integral of the Breit-Wigner transparency 6 yielding

$$G(E_{dot}, T) \approx \frac{G_0}{\cosh^2(\Delta_T)}, \quad \Delta_T = \frac{E_{dot} - E_F}{2k_B T}, \quad G_0 = \frac{\pi g_0}{4k_B T} \frac{\Gamma^r \Gamma^l}{\Gamma}, \quad (9)$$

where Δ_T is offset from the resonance energy from the Fermi level in units of $k_B T$. The relationships 9 between the conductance G and the tunneling broadening Γ solve the electron transport problem for the static dot in the ohmic regime.

The concept of the static dot is justified by the fact that the dot's translational and rotational degrees of freedom vary slowly as compared to the fast motion of the electrons. The parameters E_{dot} and Γ of the scattering matrix $S(E)$ represent adiabatic variables, validated by the Born-Oppenheimer approach. An instant conductivity of a movable dot is to be computed in a phase space of the NEM oscillator's coordinates x and momenta p . The x, p point plays the role of a partial scattering channel in which the Wigner delay time of electron tunneling $\tau = \frac{\partial S(E)}{\partial E}$ is the shortest time scale. The marginal delay τ justifies the picture of an instant scattering, where the current is obtained by averaging over the phase space. This reasoning will thread throughout this chapter after a short discussion of the proximity effects and electron balancing flows in Sec. 3.

The proximity effects and dissipative tunneling. If the dot sticks to a metal lead and forms an "adatom", its energy levels E_{dot} get broadened by hybridization with the surface continuum states. Since the electron affinity is different for the dot and the host surface, the charge transfer causes a change in the electrostatic potential inside the dot and shifts the energy levels by a contact potential. The result is that the adatom could be directly charged classically, by the electrons flowing in and out of the conduction bands. For example, Rubidium (*Rb*) is electropositive on a gold (*Au*) surface, since its ionization potential $I_i \sim 4.2eV$ is smaller than the *Au* work function $W \sim 5eV$. But it remains neutral on an isolator, such as glass, because the bonding originates from the van der Waals covalent coupling. The dot's charging depends on conditions of "quasi-equilibrium" in the open driven system "dot + leads".

For molecular dots placed far from the surfaces, the tunnel coupling is rather weak, as compared to the mechanical and electrostatic energies. Under these circumstances, the transport is usually subject to global Coulomb blockade. When the charge attempts to tunnel, it strongly perturbs the surface states, inducing a coherent reorganization of electrons and holes generating phonons or plasmons on the substrates and leads[12]. Figure 13 shows how the Fermi-edge is disturbed due to the tunneling.

A priori, when the phonon relaxation is faster than the tunneling rates, thermodynamic equilibrium should hold at the temperature of the host reservoir. However, for the nano-junctions the local surface temperature may differ from the bulk equilibrium temperature. This is due to the Anderson orthogonality catastrophe (AOC)³ associated with interplay between the van der Waals and the electrostatic forces. The electron tunneling affects the overlap between dif-

³The notion of the OC [42] was introduced by P.W. Anderson with respect to the Fermi-edge singularity where the overlap of states which differ in the number of holes by one tends to zero in the thermodynamical limit.

ferently shifted phonon ground states of the surface. The faster the tunneling rate, the closer is the phononic overlap to zero, and that hinders relaxation of the surface temperature. AOC presents the mechanism also affecting the thermal state of the electronic reservoir due to electron-phonon coupling. In Sec. 4, from comparison of our theoretical I-V curves at different electron-phonon temperatures and the experimental data [1] we infer that AOC exists.

In Sec. 3, we make use of the detailed balance conditions for derivation of a generic expression for the mean charge of the quantum dot. We formulate the field effect on the splitting and broadening of the tunnel resonance for adiabatic evolution. Here we want to emphasize that the irreversible decay is especially important for establishing steady states in the non-equilibrium system of the dot at contact with an external infinite bath. Besides the aforementioned AOC, damping of the shuttle motion of charged particles between metallic electrodes can be related to radiative decay mechanisms, discussed long ago in the seminal paper [23] by Kazantsev and Surdutovich.

3. Current at detailed balance

The system made-up of a quantum dot and two leads of different Fermi energies experiences electron flows tending to bring the system to thermodynamic equilibrium. In the steady-state regime, the net current summed over the electrodes is zero, that is the incoming and the out-going flows of electrons through the quantum dot compensate each other. The balancing process is provided by the tunnel rates Γ^σ weighted by the Heisenberg time needed for an electron of energy E to escape into the electrode $\sigma = (r, l)$,

$$\Gamma^\sigma = \frac{\hbar}{\tau^\sigma}. \quad (10)$$

If we denote the electron distribution function inside the quantum dot by $f_{dot}(E)$, the out-flow current at energy E to the right electrode is

$$I_{out}(E) = \frac{f_{dot}(E)}{\tau^r} = \frac{\Gamma^r f_{dot}(E)}{\hbar}. \quad (11)$$

The electrons populate the level E of the quantum dot by backward transitions from the lead with an incoming flow

$$I_{in}(E) = \frac{2}{\tau^r} \rho(E) f_r(E), \quad (12)$$

occurring through the resonance window $\rho(E)$ over the time τ^r , while the factor 2 in the Eq. 12 accounts for the spin degeneracy in the Fermi sea. The difference of the in- and out-going electron flows at energy E produce the net current

$$I_r(E) = e \frac{\Gamma^r}{\hbar} [2\rho(E) f_r(E) - f_{dot}(E)]. \quad (13)$$

Analogously, the expression for the current on the left lead reads

$$I_l(E) = e \frac{\Gamma^l}{\hbar} [2\rho(E)f_l(E) - f_{dot}(E)]. \quad (14)$$

Since the detailed balance principle implies that in equilibrium the electron population of the dot has to be at a steady-state, $I_l + I_r = 0$, we immediately arrive at the relation

$$\Gamma^r [2\rho(E)f_r(E) - f_{dot}(E)] = \Gamma^l [f_{dot}(E) - 2\rho(E)f_l(E)], \quad (15)$$

which yields the distribution $f_{dot}(E)$

$$f_{dot}(E) = 2\rho(E) \frac{\Gamma^r f_r(E) + \Gamma^l f_l(E)}{\Gamma^r + \Gamma^l}. \quad (16)$$

The net current in the scattering channel E is represented as

$$I(E) = \frac{e\Gamma^l}{\hbar} (2\rho(E)f_l - f_{dot}(E)(E)) \quad (17a)$$

$$= \frac{e\Gamma^r\Gamma^l}{\hbar\Gamma} \rho(E)(f_l(E) - f_r(E)) \quad (17b)$$

$$= \frac{2e}{\hbar} \Upsilon(E)(f_l(E) - f_r(E)). \quad (17c)$$

We see that the detailed balance is equivalent to Landauer's formula Eq. 3. The generic method of the steady state regime is utilized here in order to emphasize a common meaning of Landauer's ansatz of Eq. 3 corresponding to Eq. 17c. The current flows and electronic distribution $f_{dot}(E)$ in the quantum dot are self-consistently related provided

$$Q = 2e \int_0^\infty dE \rho(E) \frac{\Gamma^r f_r(E) + \Gamma^l f_l(E)}{\Gamma^r + \Gamma^l}. \quad (18)$$

The total charge accumulated in the resonance window is a trade-off between the Fermi seas of the electrodes, allowing for the establishment of equilibrium between the continuous spectra of their conduction bands and the intermediate resonance state of the quantum dot. The steady-state kinetics refers to diverse transport problems, and it can be derived by more subtle techniques such as the density matrix approach in the framework of the Keldysh representation [24] on a closed time path [25], or the nonlinear Green function methods [26], [3]. But our aim is more pragmatic: We apply Eq. 18 in the Breit-Wigner approximation for adiabatic motion of the quantum dot and calculate the average current.

Field splitting and broadening of the resonance level. Due to the huge difference of the molecular and the electron mass, slow molecular vibrations

can be considered as quasistatic when compared to the fast electron motion. The slowness of the molecular vibrations justifies the Born-Oppenheimer adiabatic approach. This strategy provides us with a paradigm useful for consideration of electron tunneling through a movable quantum dot. By the analogy to the Born-Oppenheimer molecular terms, we use the concept of tunnel curves, representing a total electronic energy as a function of the dot coordinate in the inter-electrode regions, forbidden for the electrons. However, the massive dot could move classically in this region, thus transporting an attached electron and having a potential energy, called the tunnel curve. Note that this tunnel term, being very similar to molecular one, includes both the potential and kinetic electron energies as a function of the dot center-of-mass coordinate x .

Having this in mind, the tunnel term can simply be regarded on phenomenological grounds. From the other hand, the quantum-mechanical method of Sec. 7 exemplifies an "ab-initio" approach employed here for the calculating the tunneling current. The tunnel term's topology defines the adiabatic dot dynamics and the average position of the measured electron. Thus, the averaging of the instant scattering S-matrix or the resonance transparency $\Upsilon(E(t))$ over the adiabatic paths becomes a basic ingredient of the electron transport problem.

Without loss of generality, we set the resonance energy level ε_0 equal to the Fermi energy, $E_F = \varepsilon_0$. In equilibrium, the dot assists the tunneling in remaining neutral, since the electro-chemical potentials of the leads and the dot are identical. The self-consistent "electro-chemical" potential for charging is $U_{mean} = U_c(Q - Q_0) = 0$, where U_c is the Coulomb energy cost per one electron, and $(Q - Q_0)$ is an extra charge with respect to unbiased electronic reservoirs. To estimate the field effect we write down the mechanical and electrostatic energy E_{dot} as follows

$$E_{dot} = \varepsilon_0 + U_{mean} + E_{vib} + U_{ext} \quad (19a)$$

$$E_{vib} = p^2/2M + M\Omega^2 x^2/2 \quad (19b)$$

$$U_{ext}(x) = -Fx, \quad (19c)$$

where E_{vib} is the vibrational energy of the dot of mass M . The "bouncing-ball" mode consists of the kinetic part $\frac{p^2}{2M}$, and the potential part $\frac{M}{2}\Omega^2 x^2$, with Ω being the vibration frequency. The external field force is $F = eV/D$, where D is the tunnel (inter-electrodes) gap, and V is the bias voltage.

If discharging and relaxation are faster than charging, the quantum dot remains neutral. The main role of the intermediate quantum dot is to assist a virtual tunneling through its resonance state. The quantum dot in a simple harmonic model just oscillates over a closed trajectory having the coordinate and momentum

$$x_n(t) = x_{n0} \cos(\Omega t), \quad p_n = p_{n0} \sin(\Omega t),$$

where the $x_{n0} = x_0\sqrt{2n}$ and $p_{n0} = p_0\sqrt{2n}$ are integrals of motion of n -th vibrational energy eigenstate. The zero-point amplitude and momentum

$$x_0 = \sqrt{\frac{\hbar}{M\Omega}}, \quad p_0 = \frac{\hbar}{x_0}$$

correspond to the vibrational ground state. By denoting the frequency shift due to external potential field as

$$\nu_n(t) = \frac{Fx_n(t)}{\hbar},$$

we count off the dot energy levels $E_{dot}(t) = \hbar(n\Omega - \nu_n(t))$, from the resonance reference point $\varepsilon_0 = E_F$. The detuning frequencies $n\Omega - \nu_n$ define the energy positions of the transparency resonances, required for calculation of the instant electron current by the Landauer's formula Eq. 3. A thermodynamic average of the electron transport over the dot vibrations has to be taken in order to obtain the mean current and to compare the calculated I-V curves with experimental current-voltage characteristics.

At increasing voltage, the coupling between the dot and the leads tears the phonon temperature away from the equilibrium temperature T . Thermalization of this driven open system involves complicated dynamics of the electron-phonon interactions. As an estimate, we use the Callen-Welton theorem in order to represent the fluctuation-dissipation relation between the noise power and the effective temperature of the system "leads+dot". On the one hand, the Johnson noise⁴ reads

$$S_{Jonh} = 4k_B T G, \quad (20)$$

where the G in the right hand side of Eq. 20 is the conductivity [18]. The parameter T has the meaning of an effective temperature T_{eff} for the non-equilibrium system. On the other hand, the voltage V produces the Schottky's noise that gives the main contribution to the power spectrum at a low temperature, except of the transparency resonances [18]

$$S_{Schottky} = 2eI, \quad (21)$$

where Ohm's law reads

$$I = VG.$$

By equating the power spectra of the thermal noise and the non-equilibrium shot noise

$$S_{Jonh} = S_{Schottky},$$

⁴the fluctuations at thermodynamic equilibrium are related in a universal way to the kinetic response according to the fluctuation-dissipation theorem (FTD)

we immediately relate the effective temperature T_{eff} with the voltage V , which drives the current and heats the SET to the temperature

$$k_B T_{eff} = \frac{eV}{2}. \quad (22)$$

This fundamental relationship has been obtained from the density matrix of the quantum point contact coupled with mechanical oscillator in [27]. Therein quantum heating and damping of the oscillator manifest themselves in an induced quantum-classical transition. In fact, our simple FDT arguments also indicate that heating by the electron-phonon interplay can be much larger than heating by the thermal reservoirs. The source-drain voltage V adversely affects the current and may result in undesirable artifacts, such as electro-migration, SET disruption, etc. Therefore, a non-demolished experiment requires a small voltage and low temperature, where the adiabatic approximation holds. In this limit, we can ignore the dependence of tunneling probability Γ both on the energy E and the coordinate x , setting $\Gamma \sim \Gamma_0$ near $x = 0$, since $\gamma x_0 \ll 1$. For the coherent model, the instant value of $\Upsilon(E, t)$ is given by

$$\Upsilon(E, t) = \frac{1}{Z} \sum_{n=1}^{\infty} \frac{\Gamma_0^2 e^{-\frac{\hbar n \Omega}{k_B T}}}{(E - E_d(n, t))^2 + \Gamma_0^2}, \quad (23)$$

where $Z = \sum_{n=1}^{\infty} e^{-\frac{\hbar n \Omega}{k_B T}}$ is the vibrational partition function. The path averaging yields the mean transparency

$$\overline{\Upsilon(E)} = \frac{\Omega}{2\pi} \oint dt \Upsilon(E, t) \quad (24a)$$

$$= \frac{\Gamma_0}{Z} \text{Im} \sum_{n=1}^{\infty} c \text{sgn}(c) e^{-\frac{\hbar n \Omega}{k_B T}} [(E - \hbar n \Omega - i\Gamma_0)^2 - 2n(\hbar \nu_0)^2]^{-\frac{1}{2}}, \quad (24b)$$

where $c \text{sgn}(c)$ [45] denotes a signum function of complex argument $c = e^{-i\phi}$, and $\phi = \arg(E - \hbar n \Omega + \sqrt{2n\hbar \nu_0} - i\Gamma_0)$ is used to keep continuity of the square root of the complex-valued function. The root function originates from the uniform distribution of the particles along the adiabatic path in the phase space x, p . The main contribution to the resonances gives the phase space sector $p = 0$, since the electron has a higher probability to scatter off the "static" dot, than at the dot moving in-between the turning points. The shifted frequencies ν_n are maximum at the turning points, that provides the doublet splitting of the vibrational resonances $n\Omega$. Since the frequency shift depends on the x_n , the spectral broadening increases with the vibrational energy $n\Omega$. The inset in the figure 1 shows the resonance transparency 24b averaged over the dot path.

In order to make comparison with the experiment [1], we chose the frequency $\Omega = 5 \text{ meV}$, which corresponds to a C_{60} quantum dot interacting

with gold electrodes via the Lennard-Jones potentials. For the electron temperatures $k_B T = 0.4 meV$, the vibrational amplitude is $x_0 \sim 0.03 \text{\AA}$, and hence only the zero-point mode is active, provided $\Omega \gg k_B T$. The equilibrium distance $D/2 \sim 6.2 \text{\AA}$ separates the center-of-mass of the quantum dot from both leads. When $eV \leq \Omega$, the frequency shifts ν_n are negligible, since the system "leads+dot" is cold $k_B T \ll \Omega$, and therefore $\nu_n = F x_n = \Omega x_n / D \ll n\Omega$.

However, on average, the current through the vibrating dot differs significantly from the "static" dot transmission. At growing effective temperature 22, the bouncing-ball mode produces *an inhomogeneous* broadening. This field effect results from averaging over the frequency shifts $\nu_n(t)$ that depend on the location of the quantum dot bouncing between the electrodes via the source-drain voltage characteristic, while the tunnel coupling broadens the resonance line *homogeneously*.

The Breit-Wigner approximation allows one to represent the resonance tunneling spectrum as superposition of Lorentzian lines. In the limit of narrow electronic levels $\Gamma_0 \rightarrow 0$, the resonance transparency obeys the equation

$$\overline{\Upsilon(E)} = \frac{\Omega \Gamma_0}{2Z} \sum_{n=1}^{\infty} \oint dt \delta(E - E_{dot}(n, t)) e^{-\frac{\hbar n \Omega}{k_B T}} \quad (25a)$$

$$= \frac{\Omega \Gamma_0}{2Z} \sum_{n=1}^{\infty} e^{-\frac{\hbar n \Omega}{k_B T}} \left. \frac{dt}{dE} \right|_{E=E_{dot}(n, t)}. \quad (25b)$$

This equation states that the resonance transparency of trapped dots, atoms or molecules, is formed in the neighborhood of the turning points, where $\dot{E} = 0$. At these points, $p = 0$, and the resonance transparency $\Upsilon(E)$ becomes infinite in the limit $\Gamma_0 \rightarrow 0$. However, the coupling with the environment produces a finite broadening Γ that negates the divergence of the transparency $\Upsilon(E)$.

4. Current Voltage Curves

The adiabatic treatment of the dot's motion can be used to clarify as yet unexplained features in the experimental I-V curves [1]. To this end one not only needs to find the adiabatic paths but also to perform averaging over their thermal perturbations. In our first example, the electron reservoirs are strongly coupled with the dot vibrations that are characterized by the effective temperature $k_B T_{eff} = eV/2$. The quantum dot can locally heat the surface of the leads up to the same temperature $T = T_{eff}$. The reason behind the anomalous electron heating is the electron tunneling perturbing the surface. The local quasi-particle perturbations, e.g. plasmons, cannot relax fast because of the AOC. The surface plasmons create no overlap between the shifted phonon states. As a result of phonon-plasmon interplay [12] the electron temperature T equilibrates with the phonon temperature T_{eff} .

The electronic current versus the source-drain voltage shown in the figure 1 displays the typical features of C_{60} SET [1] at the open gate $V_{gate} \ll \Omega$. At

Figure 1. The I-V curve at the same temperatures of electron and phonon reservoirs due to the AOC effect. The inset shows the doublet spectra caused by vibrating the dot with $\Omega = 5\text{meV}$ and T_{eff} at the end point of the I-V curve.

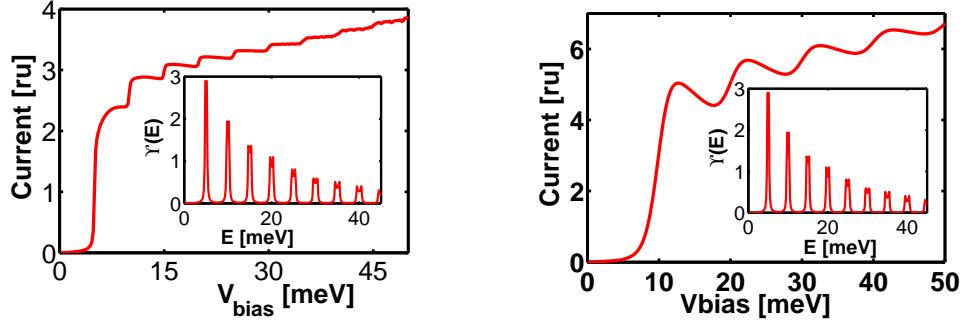


Figure 2. The I-V curve of "dot+leads" system at the equilibrium electron temperature $k_B T_e = 0.4\text{ meV}$, but at a different effective phonon temperature $k_B T_{ph} = eV/2$.

a small gate voltage, surface charge [12] is allowed, and the AOC mechanism may take place. For the C_{60} SET, the phonons manifest themselves in the step-plateau-like current, with the conductivity gap corresponding to the phonon frequency $\Omega = 5\text{meV}$, and with a negative differential resistance (NDR) regions.

The NDR can be explained by the field effect, which splits the resonance scattering lines because of the frequency shifts at the turning points, and therefore the electron flow only partly contributes to the current. In accordance with the Pauli principle, the Fermi energy spectrum window given by the difference of Fermi functions results in a step-like increase of the current, when being overlapped with the transparency resonance at the bias voltage equals a multiple of the phonon quantum $n\Omega$, as shown in Fig. 1. Since the transparency doublets are split faster than the Fermi windows are broadened out, after a step-like increase the transmitted current slightly decreases with the increasing voltage V , until the next vibrational quantum, $n + 1$, provides an additional channel for tunneling.

As the second example, we consider a model of the C_{60} SET at a large gate voltage V_{gate} that stops the tunneling current. The V_{gate} eliminates the AOC and eliminates the charge disturbances at the lead surfaces. Under these conditions, the local electronic reservoirs remain at the equilibrium temperature $k_B T \sim 0.5\text{ meV}$. If the Fermi distributions of electrons (see Eq. 3) have sharp edges at $E = eV/2$, the step of the current occurs when crossing the tunneling resonance $E = \Omega$ at $eV = 2\Omega$, (see Fig. 2). The conductivity gap at double frequency 2Ω has been observed in Berkeley [1] by measuring the differential

conductance $\partial I/\partial V$ at the frequency domain far from the bouncing-ball and the breath modes of the C_{60} transistor. The crossover regime to the 2Ω frequency has been found at large V_{gate} that suppresses the current through the C_{60} transistor, as shown in Fig. 2 on the right hand side of the $\partial I/\partial V$ plot [21]. On the contrary, a small V_{gate} opens the transistor. Then, the current produces a heating of the electronic reservoirs that smears the 2Ω line.

The present scattering theory seems to work reasonably well, considering its simplicity. The adiabatic picture explains the major features of the I-V curves and especially their NDR behaviour, displayed in the Figs. 1 and 2. The bias voltage therein is below of the Coulomb energy, and the charging of the quantum dot can be disregarded. But the broken Coulomb blockade is the basic tenet of the electron transport, whose current growth can be related to the electron affinity of quantum dot at $eV_{bias} \sim U_c$. In the next section we demonstrate that the sequential tunneling can affect the quantum dot paths by breaking symmetry of the adiabatic potential.

5. Charging and discharging in adiabatic theory of Coulomb blockade

From the detailed balance we have learned that the charging is a trade-off between the broadening Γ and the equilibration of the electron flows. The source-drain voltage can result in a sudden change of this balance and the corresponding current. Indeed, turning on the shuttle can maximize the transparency and hence the conductivity. It can also affect the noise characteristics. Qualitatively new effects such as low-frequency coherent oscillations, electric echoes, and quantum entanglement may arise due to coherence of the charge states.

In order to pick up a charge from the electronic terminal, several mechanisms have to be involved in parallel. One- and many-body effects (tunneling, screening, AOC etc.) are among them. Earlier, considering the proximity surface effects, we have noticed that in the equilibrium conditions the dot charge depends on the contact potential. This is ensured by the electrochemical potentials μ_σ $\sigma \in (l, r)$ and μ_{dot} in the leads and the dot correspondingly, when these subsystems do not interact and can be considered separately. The difference of the electrochemical potentials creates a driving force for the electron flow, which obeys the detailed balance conditions. The dot charges positively or negatively, depending on whether μ_{dot} greater or less than μ_σ , and it remains neutral when $\mu_{dot} = \mu_\sigma$.

Accordingly, the formulas for current and self-consistent charge employ the electro-chemical potentials for the control of the electron distributions in the leads and dot. The electro-chemical potentials of the electrodes are defined as $\mu_\sigma = E_F \pm eV/2$, where E_F is the Fermi energy of electrons (including

the self-energy of pair interaction) and V the external potential. The electrochemical potential $\mu_{dot} = U_{mean}(x, p)$ is characterized, in turn, by the electron affinity given by the charging potential $U_{mean}(x, p)$ so that the electronic energy of the quantum dot is

$$E_{dot} = E(x, p) + U_{mean}(x, p), \quad (26)$$

where $E(x, p)$ is the energy of the resonance electron level. For the quantum dot between leads, the role of electron affinity and ionization potential are played by the LUMO and HOMO state energies, respectively. For the self-consistent electron interaction, the mean-field potential $U_{mean} = U_c(Q - Q_0)$ denotes the charging (discharging) energy. The coefficient U_c is the cost of Coulomb energy when the dot gains (loses) one electron, Q is the self-consistent charge and Q_0 is the background charge, respectively. In the microscopic description, calculation of the mean Coulomb energy relies on the Hartree-Fock terms. The Coulomb energy integral depends on the wave-function overlap accounting for the electron-electron interactions between the electronic reservoirs and the dot.

This overlap measures the rate of tunnel transitions that entails the detailed balance condition for the SETs. The transition dynamics fall into the generic class of two-level-band systems [28]. According to the common quantum-mechanical rules [29] we identify the following cases:

- Coherent tunneling via the virtual state of the dot: The resonance level assists instantaneous transitions between electrodes, while the resonance state remains empty.
- Sequential tunneling via the real state of the dot: The dot charge is not exhausted on the time scale of adiabatic dynamics ⁵. The charge transport could be driven by actual shuttling.

Virtual and real tunneling transitions between the leads are similar, in a sense, to Raman scattering and resonance fluorescence for optical transitions. The critical dependence of the shuttling on the bias voltage, that counteracts the relaxation due to itinerant electrons and other dissipation mechanisms, implies the importance of the latter for the onset of the steady-state regime. This is similar to Vavilov's rule in optics, stating that transitions through a real state are characterized by their quenching ability. This analogy holds true for resonance tunneling, in which the electron states and transitions are treated quantum mechanically, while the adiabatic dynamics may remain classical. The notion of the shuttle instability is related to the dynamical symmetry of the bond potential (attractor) called as the tunnel term, in which the dot resides. The critical

⁵e.g. by occasional hybridization with the surface impurities.

dependence of the tunnel term on bias voltage is demonstrated below in the framework of a phenomenological approach. The quantum description of the voltage-driven bifurcation is briefly sketched in Sec. 7.

In the Breit-Wigner approximation, the charging - discharging transitions are accounted for by the offset of the energy (or the frequency shifts) dependence on the dot location relative to the leads. According to Eq. 19a it is

$$E(x, p) = \varepsilon_0 + E_0(x, p) = \varepsilon_0 + K_{in}(p) + U_{pot}(x) + U_{ext}(x). \quad (27)$$

The first part of the energy $E_0(x, p)$ is the kinetic energy $K_{in}(p) = p^2/2M$. For the matter-field interaction, this energy produces the well-known Doppler effect of inhomogeneous broadening of optical transitions. The second part is the interaction with electrodes, i.e. the Lennard-Jones potential near the equilibrium point $x_0 = 0$ taken in the harmonic approximation as $U_{pot}(x) = M\Omega^2 x^2/2$. The third part is the electrostatic interaction of the dot electron in the external field between the electrodes

$$U_{ext}(x) = -Fx.$$

In order to formally compute the mean charge during the resonance tunneling, we substitute the dot energy Eq. 26, 27 into the steady-state condition Eq. 18. This yields

$$Q(x, p) = \frac{1}{\pi} \int_0^\infty dE \frac{\Gamma^r f_r(E) + \Gamma^l f_l(E)}{(E - E_{dot}(x, p, Q))^2 + \Gamma^2}. \quad (28)$$

The Franck-Condon principle implies locality in phase space x, p . It states that the coordinate and momentum of a massive dot stay unchanged during the electron transitions, i.e. electron tunneling in our case. For detailed balance, the tunnel coupling Γ_σ has to be invoked as the main prerequisite for the Coulomb blockade. The additional relaxation due to molecular collisions and electromagnetic radiation may have to be favored for the steady state. This is similar to the dissipation necessitated in the orthodox theory of the Coulomb blockade [43], [44].

The shuttling [7] also requires Coulomb blockade, which is a combined effect of the single-electron charging and the quantized spectrum of a bound system. The charging is produced by the bias voltage V_{bias} , and hence it can be accompanied by a shuttle instability with threshold behaviour. The physical meaning of the criticality is shown to be the Landau bifurcation of the bonding potential. The vibrational energy, the temperatures, and the charge dissipation prevent the shuttle mechanism taking effect before the threshold V_{bias} is reached.

The self-consistent charge. Mathematically speaking, we have arrived at a nonlinear integro-functional equation, for which an exact analytical solution is impossible, although its analysis within physically meaningful approximations remains instructive. The integral over the spectrum corresponds to the electron equilibrant flows ensued by contact with two electron reservoirs. However, when the inter-electrode distance is much longer than the Fermi length $1/\gamma$ and the dot is trapped in the middle, $\gamma D \gg 1$, the resonance window of the dot state density is extremely narrow: $\Gamma(D/2) \approx E_F e^{-\gamma D} \rightarrow 0$. Then, the integral over the continuous spectrum of conducting electrons is collapsed by the delta functions of the dot state density:

$$Q(x, p) = \frac{1}{\Gamma(x)} [\Gamma^r(x) f_r(E_{dot}) + \Gamma^l(x) f_l(E_{dot})]. \quad (29)$$

In Sec. 3 we have already used this limit of narrow levels. The resonance spectra of the electron tunneling without charging are explained by virtual transitions. For real transitions through a charge state, the convoluted integral 28 can be reduced to the nonlinear equation 29 for the distribution $Q(x, p)$. The nonlinearity emerges from the condition of detailed balance between the dot and the Fermi reservoirs f_σ , which interact via irreversible coupling Γ_σ .

The mean charge Q can be computed with the help of library routines, e.g. by using either the Newton-Raphson algorithm or a globally convergent one. The figures 3, 4 display distributions of the charge of the molecular C_{60} transistor, for which the thermal spread of the Fermi functions is much larger than the tunnel broadening $kT_B \gg \Gamma$ at bias voltages exceeding the Coulomb energy. The charge yield (shown on the plots 3, 4) is related to the mean field that detunes the dot level from the resonance. The detuning also includes the frequency shifts due to the bonding interaction in the harmonic approximation near the potential minimum. The use of the Lennard-Jones potential could be made at longer distances, where the attraction to the surface is created by the van der Waals or Casimir-Polder potentials. This 'spontaneous' interaction is relevant for the shuttle with a large amplitude of vibrations close to electrodes' surfaces.

At moderate deviations from the equilibrium, we can chose the adiabatic potential of the movable quantum dot as detailed above. The first part is the potential energy U_{pot} of the dispersion interaction in the harmonic approximation. The second part accounts for the electrostatic energy of charging. By definition, it is the minimum energy required for adding charge Q to the quantum dot:

$$U_{adiab}(Q) = U_{pot} + U_Q + U_{ext}, \quad (30)$$

where the Coulomb and the external potentials are $U_Q = U_c Q^2$ and $U_{ext} = -FxQ$, respectively. The electro-chemical potential of the dot is the difference

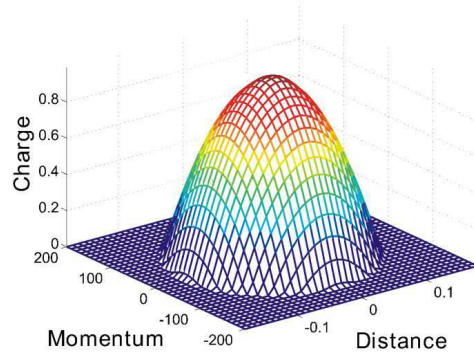


Figure 3. The charge distribution in the x and p phase space of the vibrator with the zero point oscillation amplitude $x_0 = 0.03$ and momentum $p_0 = 1/x_0$, acquires almost a Gaussian shape for a bias voltage up to $V = 100\text{meV}$.

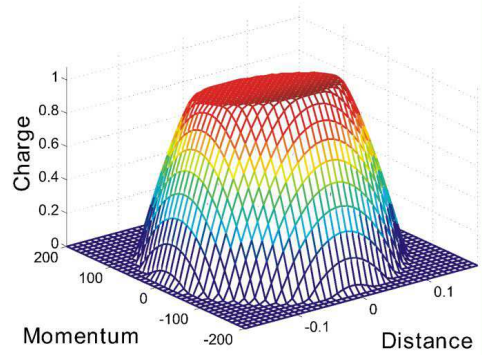


Figure 4. On increasing voltage beyond $V = 100\text{meV}$, the excess charge grows from its background value to the saturated value allowed by the Pauli principle. The saturation is characterized by the voltage bias $V = 150\text{meV}$ which is accompanied by the triple well potential.

between the adiabatic potentials of the adjacent charge states, different by one electron

$$\mu_{dot} = U_{adiab}(Q+1) - U_{adiab}(Q) = \quad (31a)$$

$$= 2U_cQ - Fx + U_c. \quad (31b)$$

The factor 2 in the electro-chemical potential of the quantum dot is to be absorbed in the mean charge Q , which accounts for the spin degeneracy in the Eq. 29. The energy U_c shifts the resonance level. Without loss of generality, we assume that the dot energy level ε_0 aligns with the Fermi energy of the reservoirs. Then from Eq. 31b, we obtain

$$U_{mean} = U_cQ - Fx.$$

for the self-consistent potential of the mean field. The adiabatic potentials modify the conductivity (see Eq. 4) in the x, p channel such that Landauer's formula relates the average charge with the average current through the quantum dot. This relationship is the central aim of any transport measurement theory. Equation 29 achieves this aim in the mean field approximation, in the spirit of the famous Weiss theory of magnetic susceptibility.

Equation 29 has two mathematical properties important for the adiabatic motion. Firstly, the dot charge in units e has, for sure, to be between zero and one. This circumstance helps one find an approximate solution in the form

of a converging power series over Q , provided $u = \frac{U_c}{k_B T} \leq 1$. On the other hand, the decomposition over exponent power e^{uQ} can be employed for $u \geq 1$. Secondly, if the thermal smearing is marginal, the dot population at the point x, p of the phase space switches quickly between the equilibrium states 0 and 1. The solution is therefore expected to be expressed in terms of the step-like Fermi functions or their derivatives.

One totally disregards the Coulomb blockade by neglecting the mean field of charging in Eq. 30. In the zeroth approximation, the $Q(x, p)$ is given by the sum of two Fermi distributions in the reservoirs

$$Q^{(0)}(x, p) = \frac{1}{\Gamma} [\Gamma^r(x) f_r(E_0(x, p)) + \Gamma^l(x) f_l(E_0(x, p))], \quad (32)$$

each of which contributes proportionally to its coupling Γ^σ with the dot. Hence the charging becomes considerable for $V \geq \Omega$, provided $V, \Omega \gg k_B T$. This means that the magnitude of the bias voltage eV has to be greater than the zero-point energy of the dot vibrations (with amplitude $x = x_0$ and $p = p_0$). Therefore

$$Q^{(0)}(x, p) \approx e^{\frac{eV/2 - E_0(x, p)}{k_B T}}. \quad (33)$$

This necessary condition corresponds to the onset of shuttling and has been

Figure 5. The tunnel terms at $\Omega = 5\text{meV}$, $k_B T = 0.5\text{meV}$, $U_c = 50\text{meV}$. The four curves correspond to $V = 0, 25, 50, 75, 100\text{meV}$. The thin lines refer to the exact numerical solution, the dotted lines to 35 without the logarithmic correction.

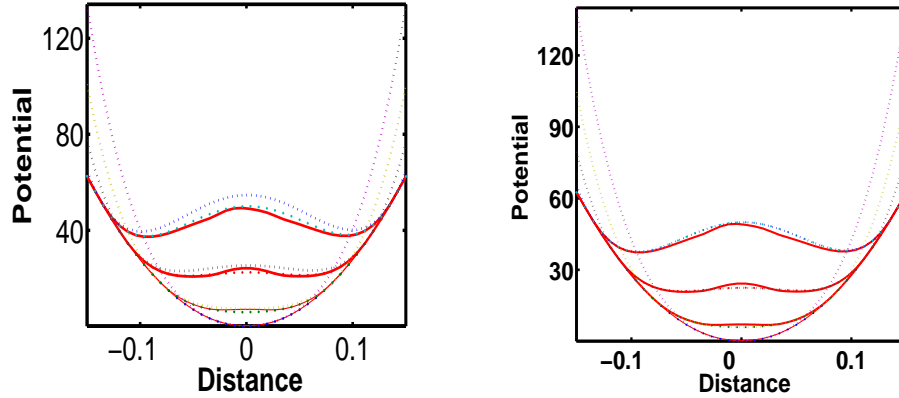


Figure 6. The same graphs but including the first logarithmic corrections for Coulomb blockade. The points on the both plots correspond to the numerical solution in the "Boltzmann" limit where the saturation of the resonance level is ignored.

found in Ref.[14]. For $u \ll 1$, however, Eq. 33 can be utilized only at the

beginning of the instability, because in this approximation the charge is independent of U_c , which does not account for the Coulomb blockade effect.

The molecular SETs are characterized by quite the opposite condition of strong blockade, $u \gg 1$, where the Coulomb energy $U_c \sim \frac{e^2}{4\pi r}$ is dominant. For instance, for C_{60} molecular radius $r \sim 3.5 \text{ nm}$, we obtain that the Coulomb energy $U_c \sim 100 \text{ meV}$ is larger than the vibrational energy $E_0 \sim 5 \text{ meV}$, and the thermal spread $k_B T \sim 0.5 \text{ meV}$. We have therefore to keep the charge Q in the exponent, instead of casting it into a power series. This approximation is equivalent to the Boltzmann limit for the Fermi reservoirs, where the saturation of population $f \sim 1$ is disregarded and the charge distribution obeys the nonlinear equation

$$Q(x, p) e^{\frac{U_c Q(x, p)}{k_B T}} = 2 \frac{\cosh(\frac{eV}{2k_B T} - 2\gamma x)}{\cosh(2\gamma x)} e^{-\frac{E_0(x, p)}{k_B T}}. \quad (34)$$

An iterative solution can be obtained with the help of a converging series of logarithmic corrections, the first two of which read

$$Q(x, p) \approx \frac{eV - 2E_0(x, p)}{2U_c} - \frac{k_B T}{U_c} \ln \frac{eV - 2E_0(x, p)}{2U_c}, \quad (35)$$

being derived from Eq. 34 under the typical conditions of molecular SET $eV \gg k_B T$, $\gamma x \ll 1$. Comparison of the approximative solutions with the exact numerical calculations of Eqs. 34 and 29, shown in Figs. 5 and 6, demonstrates the good accuracy of the Boltzmann limit. This concerns the logarithmic corrections Eq. 35 as well, until the bias voltage reaches a value of the order of the Coulomb energy, and $E_0 \sim eV/2$.

The adiabatic Hamiltonian. Dynamics of mechanical motion of the dot in x, p phase space is governed by the Hamiltonian

$$H(x, p) = K_{in}(p) + U_{adiab}(Q) = \frac{1}{2M} p^2 + \frac{M\Omega^2}{2} x^2 + U_c Q^2 - FxQ. \quad (36)$$

By substituting the eq. 35 into eq. 36 and omitting the small logarithmic correction one obtains the adiabatic potential

$$U_{adiab}(x) = \frac{M\Omega^2}{2} \left(1 - \frac{eV}{U_c}\right) x^2 - \frac{Fx}{2U_c} (eV - M\Omega^2 x^2) + \frac{M^2\Omega^4}{4U_c} x^4 \quad (37)$$

for $p = 0$, which has either a single- or double-well shape, depending on the bias voltage. The threshold voltage, at which the frequency of vibrating dot becomes zero, coincides with the Coulomb energy U_c . At this threshold, the original solution of the classical equations of motion near the potential energy minimum at the point $x = 0$ becomes instable. The bond symmetry is

Figure 7. The charge distribution (at the zero p slice) at the bias voltages at $V = 0, 25, 50, 75, 100$ meV

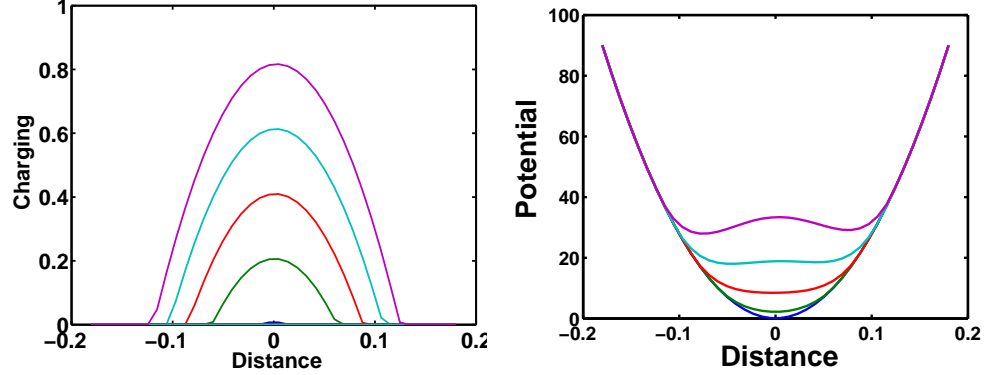


Figure 8. The adiabatic potential $U_c(Q)$ at the same voltages $\Omega = 5\text{meV}$, $k_B T = 0.4\text{meV}$, and $U_c = 50\text{meV}$.

therefore broken by the bias voltage due to the dot charging and the Coulomb blockade. The single-well potential is hence transformed into a double-well potential with new stable points locating far from the original point of equilibrium. This broken symmetry is shown in Figs. 7 and 8, obtained from the exact nonlinear Eq. 29. The figures 5, 6 also illustrate this effect in the Boltzmann limit of Eq. 34, where the analytical solution of Eq. 35 is compared with the logarithmic approximation.

Tunnel terms symmetry and phase space structure of the dot motions.

Now we are in a position to discuss the classical trajectories of the quantum dot driven by the bias voltage. To this end, the charge distributions $Q(x, p)$, plotted in Figs. 3 and 4 are substituted into Eq. 36, and the resulting adiabatic Hamiltonians in phase space are shown in Figs. 9, 10. In the thermodynamic limit, the dot tends to occupy the minimum-energy valley due to irreversible relaxation. The valley topology strictly depends on the bias voltage. The dot trajectories are running towards the center of the circle, $x = 0$ and $p = 0$, until the first threshold is reached. The source-drain voltage specified below breaks the symmetry of the single well potential (for the case of the ground state frequency $\Omega = 5\text{meV}$ it is shown in Fig. 9). The center of attraction at the point $x = 0, p = 0$ becomes unstable: The fixed points settle outside the circle, where the dot trajectories are winding. The initially compact dot distribution in the x, p phase space plane spreads into a crescent-shaped 'moon', and, then

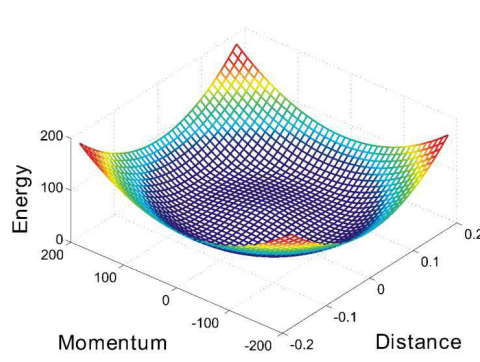


Figure 9. The energy functional $K_{in}(p) + U_{adiab}(Q)$ bifurcates into the double well potential at $eV = 100$ meV. The barrier between wells is caused by the finite cost of the Coulomb energy $U_c = 50$ meV.

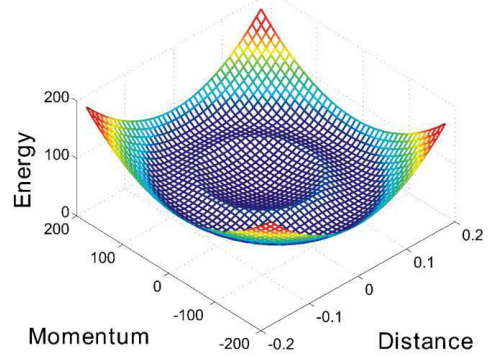


Figure 10. The voltage bias growth causes the double well to resolve into the triple well at the second threshold when the resonance state population is saturated. The saturation depends on the temperature and the Coulomb energy.

into a ring distribution of a radius found from Eq. 37 by setting

$$\frac{\partial U_{adiab}(Q)}{\partial x} = 0.$$

If the bias voltage is larger than the Coulomb energy U_c , this condition yields new stationary points of equilibrium

$$x^2 = \frac{V - U_c}{2M\Omega^2}, \quad (38)$$

corresponding to the minimum potential energy $U_{adiab}(Q)$. Furthermore, with the increase of the bias voltage the bond symmetry is broken again. The persistent Coulomb blockade produces the triple-well potential by combining the single and double wells into unified potentials as shown in Figs. 9 and 10. The multiple-well structures can not be inessential for the quantum dynamics. The coherent tunneling of electrons entails coherence between the wells, as will be discussed in Sec. 9. However, before plunging into the quantum theory we wish to turn our attention to the classical aspects of the system noise.

6. The shot noise of the shuttling instability

At the voltage threshold $V \sim \Omega$ the dot begins to oscillate with a larger amplitude between electrodes thus augmenting the current and its fluctuations. For the molecular SET, an explanation of the current-voltage steps has been attempted in terms of the Frank - Condon transitions [13]. The shuttling mechanism in the coherent regime [14] has been advocated in the works of Shekhter's

group in Chalmer's [7]. However, it seems that the kinetic models of incoherent tunneling offer the best fitting [12] of the current-voltage curves for the C_{60} SET [1].

To resolve the dilemma, one needs an additional analysis of the conduction mechanisms. For instance, the amount of electrons transported per period has been estimated on the basis of the known source-drain current $I \sim 100 pA$ [1]. However, when taking into account the frequency $\Omega \sim 1.2 THz$ of the "bouncing-ball mode", it turned out that the C_{60} transistor transmits only a small fraction $q \sim 10^{-3}e$ of the elementary charge e per vibrational period $\tau = 2\pi/\Omega \sim 10^{-12} sec$. This excess charge is too small to compete with and to affect the shuttling dynamics of the C_{60} SET.

In principle, an objection based on the broken bond symmetry model can be raised, because the frequency of dot vibrations is softened to zero at the onset of the shuttling instability. However, as shown above, e.g. 38, this could occur at a bias voltage of the order of the Coulomb energy $V \sim U_c \gg \Omega$, which is considerably larger than the observed conductivity gap Ω [1]. The current by itself cannot instruct us unambiguously about its transport mechanisms. This suggests one should try more advanced tools dealing with fluctuations rather than just with the mean current. For instance, the noise spectrum or a more general full-counting statistics could reveal more subtleties. In particular, this also concerns the Fano factor, which measures the ratio of the actual noise of fluctuation spectrum and the Poisson shot noise produced due to the tunneling of isolated independent electrons

$$F_{ano} = \frac{S_{noise}}{S_{Schottky}}.$$

This Poissonian limit, also termed as Schottky noise, has been obtained for a very low transparency $\Upsilon \ll 1$ and is proportional to the conductivity Eq. 9. We consider the resonance case, for which the dot oscillates on an adiabatic trajectory $x = A \cos(\Omega t)$ with the transparency

$$\Upsilon(\varphi) \sim \frac{\Gamma^r(\varphi)\Gamma^l(\varphi)}{\Gamma(\varphi)} = \frac{\Gamma_0}{\cosh(2A\gamma \cos(\varphi))}, \quad (39)$$

where $\phi = \Omega t$. The Schottky noise is proportional to the mean current (see Eq. 21) averaged over the dot trajectory:

$$\langle I \rangle = \frac{e^2 V}{h} \int_0^{2\pi} \frac{d\varphi}{2\pi} \Upsilon(\varphi). \quad (40)$$

The main contribution to this integral comes from the neighborhood of $\phi = \pi/2$ where the transparency is maximum, and the noise is minimum according

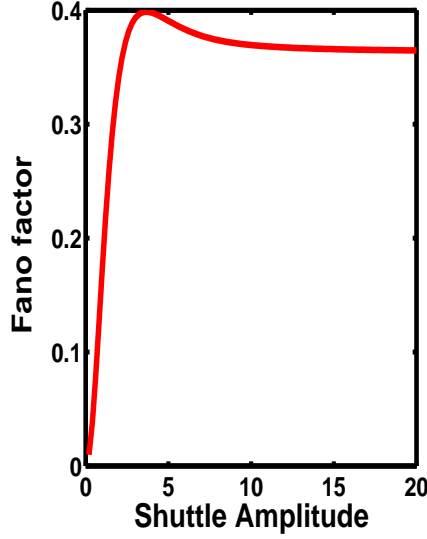


Figure 11 The Fano factor as function of amplitude A of the dot oscillation. The static dot ($A = 0$) has the resonance transparency $\Upsilon = 1$ and is characterized by zero noise. The F_{ano} -factor grows rapidly until A reaches the threshold value of $A_{thr} \sim \gamma^{-1}$ the Fermi length. After that the shuttle mechanism dominates, enhancing the transparency and correspondingly decreasing the noise slightly to keep it below of the Poissonian limit.

to

$$S = \frac{2e^3V}{h} \int_0^{2\pi} \frac{d\varphi}{2\pi} \Upsilon(\varphi)(1 - \Upsilon(\varphi)). \quad (41)$$

The Fano factor F_{ano} , (see figure 11) as a function of the shuttle amplitude is not a monotonic curve. At rest, $A = 0$, the noise is minimum for resonance tunneling since the dot energy level is not broadened and the transparency is ideal $\Upsilon = 1$. With increasing A the F -factor rapidly grows towards the threshold value $A \sim 1/\gamma$, and thereafter one is in the shuttling regime. The electron transport favors a decrease in the F -factor and augments the noise amplitude A by a value larger than the Fermi length $\lambda \sim 1/\gamma \sim 1\text{\AA}$. Figure 11 shows the Fano factor as a function of shuttling amplitude and illustrates that the better the transparency the lower the noise, as it should be for a quiet electronic sea.

This analysis shows that shuttling is hardly feasible in the reported experiments [1]. The first reason is the AOC that is caused by the tunneling at a small gate voltage. Growth of the local environment temperature destroys the Coulomb blockade, which could lead to charge accumulation and shuttled transport. The second reason is a large gating of the C_{60} transistor that removes the AOC and thermalizes the SET at low temperature $T \sim 4K$. Nevertheless, the amplitude of the thermal vibration is still too small to activate the shuttle mechanism at distances comparable with the Fermi length $\lambda \sim 1\text{\AA}$. The threshold of shuttling $A_{thr} \sim \lambda$ can not be reached even at $eV \sim \Omega = 5meV$ for the C_{60} transistor.

If zero-point vibration amplitudes of the dot are comparable with the Fermi length of the electrons, the shuttling takes place at small bias voltage. This is the case for cold dots. The constructive interference of electron waves in the tunnel gap center effectively charges the dot. In the quantum limit, this charging requires a justification of the tunnel-term concept based on the Schrödinger equation. In next section we address a more rigorous quantum mechanical picture based on the "ab-initio" SET model.

7. The Born-Oppenheimer approximation for the tunnel curves

In previous section, by considering the electrostatic energy of the quantum dot charging we have determined the tunnel curves using the phenomenological approach. A strict definition of the tunnel curves as total electronic energy at a fixed dot location between leads is implied by the Born-Oppenheimer adiabatic strategy. For the quantum-mechanical computation of the tunnel curves, the information about (1) the spatial profile of electrostatic potential and (2) the electron and ion distributions of the SET is required as an input.

The electrostatic interaction of the quantum dot with the leads is not weak due to charge images. Metallic leads screen their Coulomb interaction by creating charge holes in the electron reservoirs and by breaking the translation symmetry of the electron-electron and the electron-hole interactions. The quantum dot is subject to the dipole and multipole forces, which derive from the tunnel terms. Besides that, the screening diminishes the threshold of cold emission. The tunneling rate increases by three-orders of magnitude [47] as a result. We therefore have to consider the quantum dot and the leads as a strongly interacting combined system when computing the resonance tunneling as a function of the dot position in the tunnel gap.

The Green's function of the electrostatic field inside the double junction obeys the 3D-Poisson equation:

$$(\partial_x^2 + \partial_y^2 + \partial_z^2)G(x, y, z, x_1, y_1, z_1) = \delta(x - x_1)\delta(y - y_1)\delta(z - z_1). \quad (42)$$

The metallic electrodes are implied to be equipotential surfaces at which the boundary conditions read

$$G(\pm D/2, y, z, \pm D/2, y_1, z_1) = 0, \quad (43)$$

for all points y, z, y_1, z_1 . The solution can be represented as a sum of two components. The first one satisfies the homogeneous Poisson equation with the boundary condition provided by the voltage applied. This part gives us an external potential resulting in a Stark shift. The second part is responsible for the charging and for the Coulomb electron-electron interaction. The potential field of the charge obeys the Poisson equation, which has a delta-source on the

right hand side of Eq.42 at zero boundary conditions. The solution of the inhomogeneous equation is given by a two-fold Fourier integral. The transversal isotropy of the tunneling electron flow allows one to reduce it to a one-fold integral

$$\varphi(\chi, \chi_1) = 4e^2 \int_0^\infty d\lambda \left[\frac{J_1(\lambda a)}{\lambda a} \right]^2 \frac{sh[\lambda(\frac{D}{2} + \chi_<)] sh[\lambda(\frac{D}{2} - \chi_>)]}{sh(\lambda D)}, \quad (44)$$

which describes the field between the tips with a charge located at the point χ_1 , where $\chi_> = \max(\chi, \chi_1)$, $\chi_< = \min(\chi, \chi_1)$. Here $J_1(a)$ is the Bessel function, and the tunneling radius a equals the molecular van der Waals radius of the dot. The electron tunneling from the electrode tips occurs uniformly over a sphere of this radius. The charge density of the dipole of the length a is

Figure 12. The typical tunnel curve of the dipole dot as function of its coordinate. The source-drain voltage bifurcates at a threshold voltage: a single well is replaced by a double well followed by a wide well.

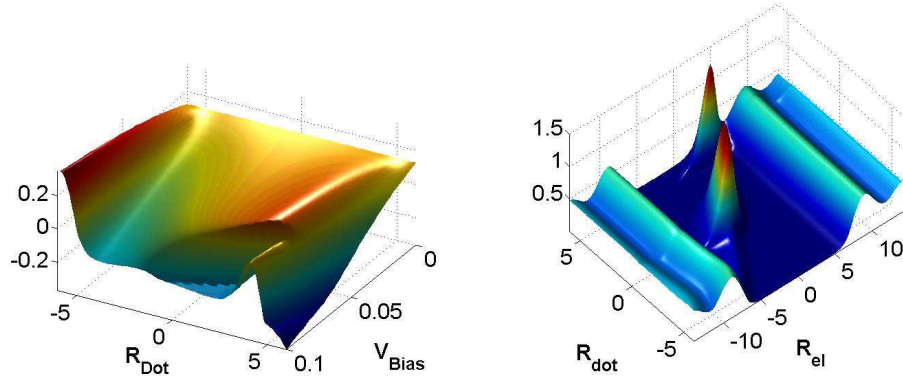


Figure 13. The electron density distribution inside SET displays Friedel oscillations at the Fermi edges and the peak of resonance tunneling in classically forbidden region in the inter-electrode gap.

$$n_d(\chi, x) = F (\delta(\chi - x + a) - \delta(\chi - x - a)); \quad (45)$$

where the $F = \alpha V/D$ and α is the dot polarizability. The electronic density $n_e(\chi, x)$ of scattering waves can be found from the wave function $\psi_{E,\sigma}(x)$ constructed from the transmitted and the reflected plane waves

$$\psi_{k,l}(x < -\frac{D}{2}) = e^{ik(x+\frac{D}{2})} + R_{k,l}e^{-ik(x+\frac{D}{2})}, \quad (46)$$

$$\psi_{k,r}(x > +\frac{D}{2}) = e^{-ik_r(x-\frac{D}{2})} + R_{k,r}e^{+ik_r(x-\frac{D}{2})}, \quad (47)$$

$$\psi_{k,l}(x > +\frac{D}{2}) = T_{k,l}e^{+ik_l(x-\frac{D}{2})}, \quad (48)$$

$$\psi_{k,r}(x < -\frac{D}{2}) = T_{k,r}e^{-ik(x+\frac{D}{2})}, \quad (49)$$

where the partial channels $k_l = k_r = \sqrt{2E + eV}$ and $k = \sqrt{2E}$ are averaged over the thermal reservoirs of the leads. This yields

$$n_e(\chi, x) = \sum_{\sigma=r,l} \int_0^\infty dE f_\sigma(E) |\psi_{E,\sigma}(\chi, x)|^2. \quad (50)$$

The net charge distribution $\rho(\chi, x) = n_e(\chi, x) - n_d(\chi, x)$ can be used for computing the energy functional of the electron-electron and electron-hole interactions in the tunnel gap. The potential energy of the induced charges as a function of the dot location is proportional to the integral

$$P_H(x) = \frac{1}{2} \int_{-D/2}^{D/2} d\chi \int_{-D/2}^{D/2} d\chi_1 \rho(\chi, x) \varphi(\chi, \chi_1) \rho(\chi_1, x), \quad (51)$$

which measures the electron and hole overlap. It is related to the rate of the tunnel transitions by the detailed balance condition between the Fermi reservoirs and the dot. The kinetic energy also depends on the dot location and can be calculated as

$$K_{el}(x) = \sum_{\sigma=r,l} \int_0^\infty \frac{dE}{2} f_\sigma(E) \int_{-D/2}^{D/2} d\chi \left| \frac{\partial \psi_{E,\sigma}(\chi, x)}{\partial \chi} \right|^2. \quad (52)$$

Both the electrostatic and the kinetic parts combine into the total electron energy. As a function of the coordinate x , this energy plays the role of a mechanical potential

$$U_T(x) = \frac{K_{el}(x) + P_H(x)}{\int_{-D/2}^{D/2} d\chi n_e(\chi, x)} \quad (53)$$

of the quantum dot in the classically forbidden region of the electron motion. This adiabatic potential is called a tunnel curve, by analogy to molecular curves in the Born-Oppenheimer theory. The tunnel curve depends on the location of the quantum dot in the tunnel gap and on the Fermi distribution of the elec-

tronic reservoirs. The electron density in the quantum dot is obtained by solving the Hartree equation for the electron wave function

$$-\frac{1}{2} \frac{\partial^2 \psi_{E,\sigma}(\chi, x)}{\partial \chi^2} + [U_{ext}(\chi) + U_H(\chi, x)] \psi_{E,\sigma}(\chi, x) = E \psi_{E,\sigma}(\chi, x) \quad (54)$$

with the boundary conditions at the electronic reservoirs, where the potential $U_H(\chi, x)$ reads

$$U_H(\chi, x) = \int_{-D/2}^{D/2} d\chi_1 \varphi(\chi, \chi_1) \rho(\chi_1, x). \quad (55)$$

One should also invoke Fermi statistics. A typical tunnel curve is shown in Fig. 12 for SET model with $D = 14 [au]$, $a = 1 [au]$, the work function of electrodes $W = 0.4 [au]$, the Fermi energy $E_F = 0.2 [au]$, and the polarizability $\alpha = 200 [au]$ (of Na atom). The potential drops near the interface of the source-drain electrodes, as it should for the ballistic regime. The tunnel curve has a single shallow well at a small bias voltage. When the latter increases, the well becomes deeper, and the dot is attracted to the inter-electrode gap center due to resonant tunneling. When the bias voltage grows further, the second well appears near the drain electrode. Then, the wells are broadened and combined into a single wide potential thus giving rise to the shuttle mechanism of conductivity, as displayed in Fig. 12. This figure justifies, in principle, the broken-symmetry mechanism discussed in Sec. 5 in the framework of a phenomenological model. The electron density as a function of the electron and the dot coordinates is plotted in Fig. 13.

Density of states and current simulation. The edge electron density is subject to Friedel oscillations due to interference between the incident and the reflected electron waves. The electrons in the conducting bands of the leads are treated within the jellium model as shown in Fig. 13. The transmitted electronic waves of the source and drain electrodes can interfere constructively on the quantum dot, which is located near the inter-electrode center of the sequential tunnel junctions. The Fermi electrons create a maximum density on the dot, provided the condition of resonance with the dot quantum level is fulfilled. This effect dominates in the tunnel gap center, as well as in close proximity to the drain electrode, which screens a negative charge more effectively thus serving as a barrier to electron tunneling. When the bias voltage increases, the resonance level of the dot may shift downward the transparency window allowed by the Pauli principle, and that may entail a negative differential conductivity in concert with suppression of the electron interference, as featured in Figs. 14, 15.

Figure 14. The current through the dipole as function of its position inside the tunnel gap and bias voltage. The maximum tunneling current is concentrated at the gap center, where constructive interference of electron flows takes place.

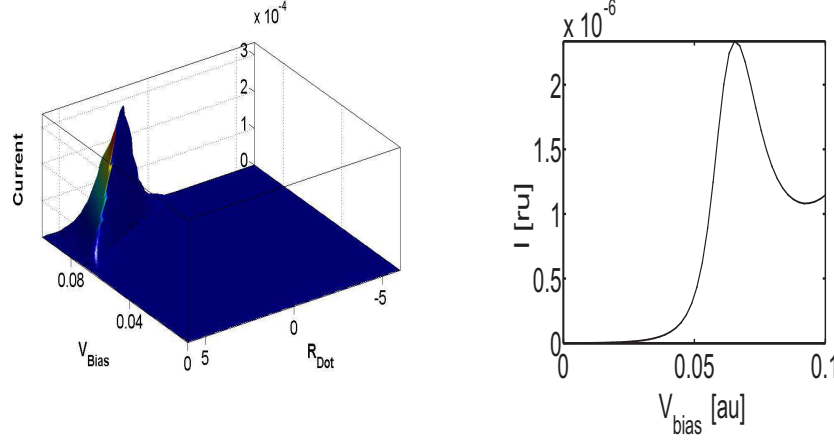


Figure 15. The current voltage curve of the tunnel transition via the dipole. Averaging it over the coordinate between the electrodes is given classically with the Gibbs distribution. The step increase of current is due to shuttling.

8. Tunneling Optical Traps

Recent progress in the atomic microchips industry, has stimulated great interest in studies of neutral ultracold gases [32]. The ultra cold atomic samples are typically produced in magneto-optical traps, then loaded into either stable microtraps or atomic guides, which employ microfabricated structures of current-carrying wires at surface substrates. These chips offer great promise for continuously improving the functioning of a variety of atomic-optic devices, including matter-waves interferometers, double well potentials for atomic Josephson junctions, and Fabry-Perot resonators for coupling cavities with atoms. However, a number of physical mechanisms stipulate fundamental limitations and hinder immediate applications of these devices.

The micro-devices require large gradients of magnetic fields for manipulation of cold atoms. Thus, large currents, up to 1 *Amp*, create significant magnetic forces in close proximity ($\sim 1\mu m$) to surfaces. Apart from collisional losses in a trapped thermal atomic cloud, strong thermal- and Johnson-noises due to current fluctuations inevitably induce additional losses, by heating and pushing atoms to the surfaces. Recently created combined magnetic and electrostatic traps [36] suffer from similar shortcomings: Up to 100 *V*-high bias voltages applied between μm -scale distant electrodes are also accompanied by

trap fluctuations that prevent an accurate deposition of the atoms close to the electrode surface.

Figure 16. The schematics of tunneling optical trap (TOT): the evanescent field of the blue detuned light repels the atoms from the laser irradiated substrate and the electrical terminals.

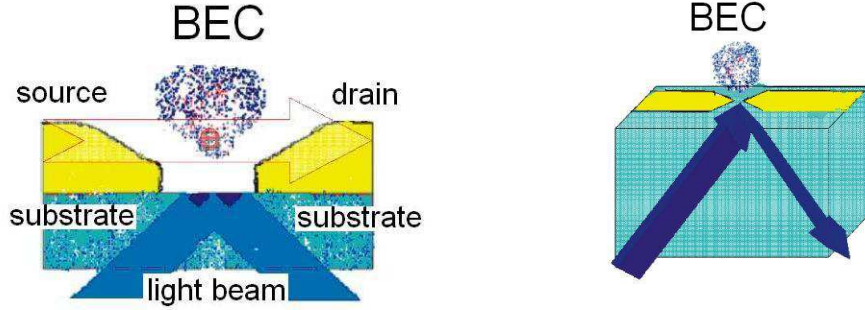


Figure 17. The current carried by terminals on the surface tend vice versa to attract the atoms to the inter-electrodes zone of maximum field. The TOT current is easily controlled by the evanescent light that plays the role of the gate electrode.

Theoretically, the electro-optical trapping (TOT), shown in Figs. 16, 17, is a much more appealing scheme for maintaining and manipulating atoms as compared to the MOT, since the electric coupling dE_s or $e\phi$ in such traps does not involve the atomic fine structure and is much stronger than the magnetic coupling. This reduces by many orders of magnitude the required voltage applied between the electrodes in order to create a trap of a same depth. Moreover, the TOT is free from the Majoranna spin-flip losses. These facts could enable one to eliminate the most of noises⁶ and to improve the trap control.

Contemporary standards for labs and industry require construction of TOT in planar geometry based on the evanescent laser fields. The dipole potential for evanescent waves reads:

$$U = -0.5\alpha_s E_s^2, \quad (56)$$

where the sign of the polarizability α_s depends on the sign of the detuning from resonance. At blue detuning, the field tends to expel the irradiated atoms from the region with high intensity of the light (see appendix). The advantage of blue detuning the evanescent field is that the atoms spend most of the time in the field-free region, and hence they are less affected by spontaneous radiation

⁶The smaller the current and voltage applied, the smaller the Schottky shot noise.

and heating. The attraction of atoms to the tip's neighbourhood is due to the electrostatic source-drain field. The separation $0.1-10\mu m$ between the source-drain electrodes allows the elimination of leakage currents and to facilitate cooling by electron transport through the resonance states of the TOT atoms.

Up-to-date techniques of cooling, including radio-frequency evaporation, optimal control of current, degenerative feedback, and, last but not the least, adiabatic laser cooling [40], have been purposely developed, and now they enable one, in principle, to maintain the ultra-cold atoms in a TOT. Sisyphean cooling by the blue-detuned light may provide the required dissipation in the TOT and further reduce a diffusive heating produced by the electron current and atomic collisions. With the repulsive light forces, which push atoms towards the dark regions near the trap center where the radiation losses should be minimal, the cold atoms can be significantly compressed adiabatically, thus yielding a background-free sub-10-nm spot [41]. In addition, constructive electron interference in these regions provides a maximum transparency of the resonant tunneling, which is required in order to minimize losses due to current driven heating of the atomic cloud.

Moreover, delivering the already cooled atoms close to the surface does not pose a serious problem. The most routine method of loading is cold-cloud transport directly from MOT to TOT. Loading atoms on the fly by photodesorption from the surfaces of a glass cell has been demonstrated recently [39]. In order to minimize radiation heating and collisional losses, the ultra cold atoms can be isolated in a dark spot near the tunnel gap leads and the substrate. In fact, a thermal cloud exhibits loss at a distance larger than the size of a compact condensate, because the proximity to the surface can provoke cloud evaporation [37]. Then, the interface can be used to selectively absorb higher energy atoms. Recent MOT experiments [32] demonstrate that by tuning the potential it is possible to bring ultra-cold atoms to a distance $0.5\mu m$ -close to the surface. This is the case where the TOT can manifest its excellence.

In addition, the evanescent field of the TOT is concentrated near the electrode apex, thus providing an additional gain in repulsion of the cold atoms to the dark spot between the electrode tips. Therefore, the TOT protects the quantum dots better against surface losses. Moreover, if the de Broglie wave length of atoms is larger than the correlation length of the surface roughness, reflection of the cold remnants occurs elastically. A movable quantum dot starts to oscillate, being trapped between the voltage biased tips. The adiabatic dynamics, in which the repulsion of the evanescent laser field compensates the electrostatic attraction to the tips, mimics Franklin's Bell oscillations with the shuttling mechanism of conductivity through the charge BEC.

The strength of attraction between the dot and the source-drain electrodes depends on the ground state polarizability, α_s . For example, the α_s is about $80[mHz/V^2/cm^2]$ for Rb^{87} . For a μm -scale inter-electrode gap, $D \sim 1\mu m$,

the voltage bias $V \sim 30mV$ produces an external field pulling the atoms into a $U_{trap} = \alpha_s(V/D)^2 \sim 8$ KHz-depth trap. For an atom de Broglie length $\lambda_{dB} \sim \hbar/\sqrt{2MU_{trap}} \sim 0.1\mu$ and a trap size of the order of D , we expect that approximately $N = (D/\lambda_{dB})^3 \sim 10^3$ atoms can be put into the quantum degenerate regime, provided their protection against sticking and colliding with surfaces is efficient. The repulsion potential of the atoms is due to the blue-detuned evanescent field. The corresponding dipole force compensates for the electrostatic attraction of the charged ultra-cold particle to the leads and to the substrate.

The density of the atoms, which should approach the leads as close as possible without sticking, significantly influences the TOT resistance R . Therefore, the repulsion of atoms has to be controlled by the attenuation of the evanescent laser field. Typically the laser beam of $1 - 100mW$ power can be focused on the interface to allow ultra-cold atoms to levitate above it.

Levitation of Cs atoms in the evanescent field has been demonstrated in [33], where the optical dipole potential created by $1W$ -laser has been utilized for trapping the atoms far from the surface. The exponential profile of the potential decreases at a half-wave length $\lambda_{blue}/2 \sim 250nm$. At these distances the optical field compensates for the long-range attraction induced by the electrostatic polarization and the Casimir-Polder potential

$$U_{Casimir-Polder} \simeq \frac{c_4}{R^4}, \quad c_4 \sim 1 [nK \mu m^4]. \quad (57)$$

which exists owing to spontaneous electromagnetic field fluctuations for neutral atoms and ensures the existence of a stationary point in the net potential field. The Casimir-Polder interaction for a Rb^{87} atom located at a distance $\sim 0.5\mu m$ from the surface is equal to the polarization potential Eq. 56 induced by $15mV$ voltage of the source-drain terminals. The surface repulsion due to the evanescent field is of the same order of magnitude for other alkali atoms K, Na, Rb , provided the corresponding matter constants and the optical wave lengths are taken into account. For the reader's convenience, in an Appendix we quote the formula for the dipole potentials in the laser field.

Both the optical and the electrical trapping have already been demonstrated separately. The double evanescent wave trap for atoms has been proposed in [30] and has been demonstrated in [33] for Cs atoms. Bezryadin and coworkers [31] have reported a method of fabrication for nanoscale controllable break junctions, in which the polarized nano-clusters, such as Pd clusters, have been trapped between the electrodes. The nano-clusters were self-assembled in the region of the maximum field in order to produce a wire connecting the tips [31].

Both types of trapping, by optical and by electrical potentials, eventually can be combined into a common protocol of cross-coupling ultra-cold atoms and electrical circuits. Such a cross coupling of the electron current and the

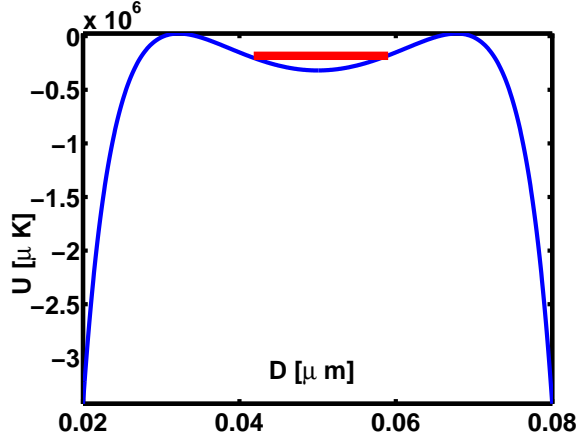


Figure 18 Schematics of the electro-optical potential including the Casimir-Polder attraction of eq. 57 for Rb^{87} atom between leads. The evanescent field, that decreases exponentially on its half wave-length expels atoms away from the surface to the location where attractive forces balance the light pressure. The line in the well cartoons the trap occupation.

ultra-cold atoms in matter wave-guides is proposed here using the example of hollow optical fibre guiding. In this scheme, a laser field, detuned either to the blue or to the red wing of the atomic transition, allows the atoms to be guided through the fibre capillary. The technique has already been routinely used [38].

Here we suggest that experimentalists address the ultra-cold metallic gas cloud in the capillary channel *electrically* in order to measure a tunneling I-V curve. To this end, the voltage bias could be led to the cold cloud through a lateral wire, which crosses the bulk of the optical-guide wall and immediately breaks-off inside the capillary. The blue-detuned evanescent field repels the ultra-cold atoms towards the capillary axis. The ponderomotive field potential accelerates the tunneling electrons and facilitates charging of the trapped atoms. This scheme features an effective reduction of the collisional loss and protection from leakage of currents. The optical field protects the electrical reservoirs of the source-drain leads from any disturbances by tunnel electrons. The last but not least advantage is that the ultra-cold atoms are trapped inside the capillary in the dark spot, which is affected neither by heating caused by the spontaneous decay nor by induced radiation processes.

The TOT scheme relying on the wave-guides also has a practical advantage over the planar design, since it requires a smaller number of microfabricated components. The heart of the setup is the quantum dot, which is created by self-assembly of the ultra-cold cloud in a dark spot between the electrodes. The self-assembly due to the optical dipole force and the electrical polarization potential is very useful for fabrication of TOT devices at such a small length scale. This scheme of cross-coupling merits a detailed consideration, since

it should allow one to discover the true electrical resistance of atomic BEC.⁷ Theoretically, the BEC collective state could be described by a composite order parameter, which is formed by the diatomic molecules and superconducting BCS pairs. It would be advantageous to map the atomic wave coherences to the coherent electric responses (echoes) of the normal or superconducting leads by applying the voltage bias to the quantum degenerate ultra-cold gas in the TOT.

We conclude this section by listing the evident TOT advantages:

- Small density of states, typical of the TOT atoms, reduces the leakage currents, the dissipative tunneling, and noises in measurements.
- High protection of atoms in the TOT from the influence of the environment favors coherence of their electrical response (nutations and echoes) to pulsed bias.
- Controllable double-, triple-, or, in principle, multiple-well potential as well as current oscillations in the atomic Josephson transitions can be achieved.
- Precise control of matter wave interferometry is foreseen.
- Combined addressing of the quantum states of the TOT both optically and electrically is possible.

In brief, we propose the TOT electro-optical setup in which electrical measurements have a high quality factor combined with the coherence of an all optical experiment. The TOT can be easily incorporated in electrical circuits as a nonlinear element ensuring a scalability of the architecture. The quantum dot isolation in the TOT will protect entanglement of quantum states thus permitting field programmable gates arrays.

9. Coherence of electron transport via double wells

Thus far we have made no reference to a wave-like motion of the NEM-SET devices. However, the coherent behaviour of the trapped quantum dots will become increasingly important with the NEM-SET made smaller and colder. The wave function Ψ formalism is useful as a description of quantum dots only when their de Broglie wavelength L_d is comparable with the Fermi length of electrons, that is $L_d\gamma \sim 1$, and we can rely on the tunnel curves. At the temperature when quantum degeneracy occurs, the self consistent charge

⁷Prof. V.L. Ginzburg once said that any synthesized atomic or molecular combination is a valid candidate in the quest for a superconductive state.

Eq.18 transported through the SET junctions via the shuttle mechanism is not smeared over the tunnel terms. As demonstrated in Sec. 7 and 8, a peak of the charge distribution is centered between the electrodes and the Coulomb blockade abruptly breaks this symmetry of the tunnel term when the bias voltage $V \geq U_c$. The single-well bond then bifurcates into a double-well potential, because the barrier between the wells brings a gain in the Coulomb energy. The corresponding self-consistent charge is imposed by the condition of detailed balance between the electron flows and an irreversible coupling Γ_σ .

Tunneling of non-correlated itinerant electrons through the lead interfaces at the rate Γ_σ provides irreversible dissipation, which is required in our approach⁸ by the detailed balance condition. The electron flows charge the resonant state of the dot (see Eq. 29) thus forming the tunnel curves U_σ (where $\sigma = l, r$), provided the charge is located in the center between the electrodes. The electron scattering and tunneling are the dissipating mechanisms that ensure stability of the adiabatic dots' dynamics. The dots can also relax their kinetic energy by collisional losses, scattering, spontaneous emission, or laser cooling. In quantum gases, binary scattering of atoms usually results in a shift of the energy level, which is proportional to the product of s -scattering length a and the gas density ρ . The interplay of the quantum spreading and scattering of the dots sitting in a single-well potential $U(x)$ is accounted for by the Gross-Pitaevskii equation for the "condensate" wave function Ψ [46] as

$$i\hbar\dot{\Psi} = \frac{p^2}{2\tilde{M}}\Psi + U(x)\Psi + \frac{4\pi\hbar^2 a}{\tilde{M}} |\Psi|^2 \Psi, \quad (58)$$

where the $\hat{p} = i\hbar\frac{\partial}{\partial x}$ is the momentum operator, the \tilde{M} is the effective mass of a dot. The scattering length a has to be smaller than the average distance between dots in the trap, this serves as a criterion of validity of the Gross-Pitaevskii equation. The quantum dispersion of the dot $\frac{1}{2\tilde{M}}\hat{p}^2$ brings about the major spreading mechanism in the degenerate quantum regime. The electron transport critically depends on the bias voltage V : For $V < U_c$ the adiabatic potential U features a single well, which for $V > U_c$ bifurcates into a double-well potential with degenerate states located in the well minima.

Should one disregard the s -scattering off a small density of states $|\Psi|^2$ in a dilute quantum gas, the resulting linear Schrödinger equation would describe the dynamics of the Ψ -state in the potential U . The Landau bifurcation then emerges from casting the potential $U(x)$ of Eq. 37 into a Taylor series over a small deviation x from the bifurcation point:

$$U(x) = \tilde{M}(\Omega^2 - \Sigma^2)x^2 + \Xi x^4.$$

⁸as well as in the orthodox theory of Coulomb blockade [43], [44]

Parameters Σ and Ξ are defined by the condition of Coulomb blockade. They depend on the temperature, the bias voltage, and the coupling to electron reservoirs, that all influence the criticality of quantum dynamics. The quantum degenerate regime is meaningful when the dot temperature is smaller than the Coulomb energy. The heat supplied to the dots by the bias voltage has to be dissipated in order to reach the degeneracy point. The required relaxation is provided by the radiation channels via the Josephson plasmons of the dot tunneling across the Coulomb barrier. The tunnel transitions split the degenerate energy levels corresponding to the dot motion in the wells' minima of the bifurcated potential. The frequency of splitting is just the Josephson frequency quantum.

Alternatively the quantum dynamics on the tunneling curve can be invoked by the wave functions Ψ_l and Ψ_r of the dots, each of which resides in its own well. The functions Ψ_l and Ψ_r obey the system of equations

$$i\hbar\dot{\Psi}_l = \hat{H}_l\Psi_l + \Delta_l\Psi_r, \quad (59a)$$

$$i\hbar\dot{\Psi}_r = \hat{H}_r\Psi_r + \Delta_r\Psi_l, \quad (59b)$$

where $\sigma = l, r$, and the quantities $g_\sigma = 4\pi\hbar^2 a_\sigma / \tilde{M}$ are related to the corresponding s -scattering lengths of the matter waves with Hamiltonians $\hat{H}_\sigma = \frac{1}{2\tilde{M}}\hat{p}^2 + U_\sigma + g_\sigma |\Psi_\sigma|^2$. Equations 59a, b can be considered as a generalization of the Gross - Pitaevskii equation of the interacting charged Bose gas. Alternatively, it can be obtained from the many-body Hamiltonian of the field theory. The mean field Hartree dynamics is presented in Eqs. 59a, b. The tunnel terms $U_{l,r}$ are modified by the collisional shifts due to s -scattering of particles in the same well. The $\Delta_{l,r}$ defined below implies the inter-wells' scattering. For the charged Bose gas the interaction Hamiltonian of the field theory reads

$$\hat{H}_{\text{int}} = \int \int \hat{\Psi}^\dagger(x) \hat{\Psi}^\dagger(x_1) \varphi(x, x_1) \hat{\Psi}(x_1) \hat{\Psi}(x), \quad (60)$$

where $\varphi(x, x_1)$ denotes the Green's function of the Poisson equation for the electrostatic potential in the inter-electrodes zone. We represent the field operator of the Bose field as

$$\hat{\Psi}(x) = \Psi_l(x) + \Psi_r(x) + \text{fluctuating fields},$$

where the average of the fluctuating part tends to zero in the thermodynamic limit. The overlap integral Δ measures the rate of particle tunneling through the barrier. The integral Δ is obtained from the variational derivative of the interaction Hamiltonian Eq. 60

$$\frac{\delta \hat{H}_{\text{int}}}{\delta \hat{\Psi}^\dagger(x)} = \int dx_1 \varphi(x, x_1) \langle \hat{\Psi}^\dagger(x_1) \hat{\Psi}(x_1) \rangle.$$

The dependence of φ on x is slow and we can disregard it as compared to the function of the difference $x - x_1$ modelled by the Dirac δ -function, so we have

$$\Delta_{l,r} \approx \int dx_1 \varphi(x_{l,r}, x_1) \Psi_r^*(x_1) \Psi_l(x_1) \approx \frac{4\pi\hbar^2 a}{M} \Psi_r^*(x_{l,r}) \Psi_l(x_{l,r}). \quad (61)$$

The two states Ψ_l and Ψ_r are macroscopically distinct if their separation is of the order of the wavelength. For instance, ultra-cold rubidium Rb atoms oscillating in a TOT with frequency $1kHz$ have a wavelength of about $1\mu m$. The coherence length limits the maximum barrier width that allows atoms to be hybridized between the wells. The model describes screening in the charged Bose gas with Josephson plasmons. The current through the degenerate quantum gas reads

$$J_l = \frac{2e}{h} \left\{ \Psi_l^* \frac{d\Psi_l}{dx} - \Psi_l \frac{d\Psi_l^*}{dx} \right\}. \quad (62)$$

The Josephson current is obtained by multiplying Eq. 59b by the conjugated wave function Ψ_l^* and integrating by parts. This yields the flow of the charged Bose gas with the current

$$J_l = \frac{2e}{h} \Delta \text{Im} \left\{ \int dx \Psi_l^*(x, t) \Psi_r(x, t) \right\}. \quad (63)$$

The overlap of the wave functions oscillates at a frequency $\Delta = \Delta_l \approx \Delta_r$. For weak superconductors, the tunneling frequency Δ is controlled by the source drain voltage. The alternating current (ac) is zero below the threshold voltage and it oscillates after the threshold with an amplitude growing with the bias voltage. Existence of ac at the frequency Δ immediately indicates the broken symmetry of the bond potential. The frequency of the current is proportional to the source-drain voltage and, thus, the SET radiates an electromagnetic field. This radiation causes relaxation that ensures a back-action mechanism for establishing an equilibrium in the composite system.

It is worthwhile to note that the charged Bose gas trapped in the double well potential U_σ of Eqs. 59 behaves as an inverted Josephson junction (N-S-S-N). The super-current, which accompanies the matter wave coherence, is induced between the degenerate resonance states of the adjacent wells at the frequency of the tunnel splitting $\Delta \ll \Omega$. While the shuttling frequency Ω cannot be displayed directly because of a large response time, as is typical of tunnel junctions (whose frequency cutoff is much smaller than the vibrational frequency even for nano junctions). The coherent oscillations of the Josephson current can be observed by virtue of their slow frequency $\Delta \sim V$ which is robustly controlled by the bias voltage.

10. Summary

The step-wise and negative differential resistance regions of the current-voltage curves observed in the molecular C_{60} transistor [1] are explained by the field effect, in which the voltage bias of the source-drain leads intensifies the NEM effective temperature. With increasing bias, the field splitting and the inhomogeneous broadening modify the transparency spectra of electron scattering. We have obtained a good qualitative agreement between our simple adiabatic models and the differential conductance observed experimentally. Our formula also displays the crossover between the internal mode (~ 33 meV) and the bouncing-ball mode ($\Omega \approx 5$ meV) of the differential conductivity in the molecular SET. With further increase of the electrostatic interaction, the shuttling mechanism of conductivity replaces the tunneling regime. Then, the Coulomb energy growth destroys the bonding symmetry of the single well potential. The broken symmetry of the molecular vibrations in back-action cures the shuttling instability. The shuttle regime is characterized by shot noise reduction and by coherence of the oscillating current. The primary quantization picture demonstrates that the current oscillates at the frequency of the ground state splitting Δ and the amplitude of this oscillation grows proportionally to Δ .

We have developed an unified adiabatic approach allowing one to tackle transport problems in traps of different geometry. The magnetic and electrical fields, charge screening, and other factors (a spin-orbit interaction, hyperfine structure, *etc*) can influence the quantum dot paths within an easily tractable Breit-Wigner-resonance approximation for the electron scattering. The utility and universality of the tunnel terms concept are confirmed for the phenomenological and 'ab-initio' theories of the shuttling instability.

The shuttling in a quantum gas is relevant to electron transport in the presence of relaxation and the Coulomb blockade. The Coulomb blockade entails broken symmetry of molecular potentials U_σ ($\sigma = l, r$) when a single well bifurcates into a double well. Tunneling of the charged Bose gas in a double well between biased electrodes creates a current which is subject to Josephson oscillations. This ac generates an electro-magnetic field and thus providing an additional mechanism of dissipation. Thence, the broken symmetry and coherent oscillation due to molecular vibrations ensure the necessary and sufficient conditions legitimizing the present scenario of bond bifurcation.

The adiabatic theory of electron transport in the Breit-Wigner approximation may be of more than academic interest. It can help one to devise the TOT protection of the NEM - SET systems against decoherence. The TOT technology is better suited for molecular optoelectronics due to a low noise in combination with protection control. The connection between the TOT conductivity and quantum Franklin's Bell paradigm is discussed. The TOT design

for avoiding the dissipative "roadblocks", could serve as a road map toward a new generation of optical SET, that should enable electrical non-demolition measurements on the quantum threshold. It would be of great interest to measure the resistance of a TOT comprising of BEC molecules and BCS atomic pairs.

Acknowledgments

With the present paper we pay a tribute to our friend and teacher A.P.Kazantsev. He made the seminal contribution to the now enormous field of activity of mechanical action of light on neutral atoms. He often prophesied the future development for years ahead. Four decades ago he recognized the significance of radiation from accelerated charged particles near metallic surfaces [23] that appears to be of importance for dissipative mechanisms in TOT electron transport.

The authors are indebted to colleagues for numerous discussions. In particular we thank A.Bezryadin for his preprint [31] which he sent to us, to I. Novobrantsev for keen interest and encouragement, and G.Surdutovich for his valuable remarks and references. We are thankful to RFBR and the program of scientific schools for the financial support. The hospitality of INF in Ferrara (Italy) is greatly acknowledged by one of the authors (A.R.), especially, to S. Atutov and R. Calabrese for a kind invitation. The collaboration with the experimental team at the winters 2000-2001 has led to the ideas developed therein.

GLOSSARY

AOC Anderson orthogonality catastrophe [42]. Zero overlap between ground states of surface vibrations: e.g. the original state and charge induced configurations, where phonons are shifted by the tunneling electron.

BEC Bose-Einstein condensate. Degenerate state of an ultra-cold ensemble, i.e. a coherent, single-mode, bright atomic source of zero momentum $p = 0$.

MOT Magneto Optical Trap. The well established technique for Doppler cooling and trapping of a thermal cloud of cold atoms.

NDR Negative differential resistance.

NEMs Nanoelectromechanical systems. Composite mesoscopic and nanoscale devices designed for a new functionality.

SET Single-electron transistor. Double tunnel junctions with a central island serving as a gate electrode.

SSET Superconducting Single-electron transistor. The same as SET, but the bulk of the electrodes are superconducting.

TOT Tunneling Optical Trap.

Appendix: Radiation pressure

Demonstration of levitation of micron-sized latex particles by radiation pressure dates back to 1970 in the experiments reported by Ashkin [34]. The average force accelerating (or slowing down) atoms in a laser field was derived by A.Kazantsev in 1972 [35]. Later in 1972-1974 he classified the optical forces as spontaneous, induced and mixed. In particular, it was he who first presented the dipole potentials for velocity broadened lines of resonance atoms in the logarithmic form

$$U = \frac{\delta}{2} \ln \left[1 + \frac{G^2}{\delta^2 + \gamma^2} \right] \quad (\text{A.1})$$

here $\delta = \Omega - \Omega_0$ is the detuning from resonance, γ is the atomic linewidth, Ω , Ω_0 , $G = dE$ is the frequency of light, the resonance transition and the Rabi frequency respectively, d is the dipole moment of the transition (in units $\hbar = c = 1$), and E is the laser field amplitude. At large detuning, the dipole potential takes the canonical form (Askaryan, 1962)

$$U = -0.5\alpha E^2,$$

where the optical polarization is

$$\alpha = -\frac{d^2}{\delta}.$$

This potential repels the atom from antinodes of the blue detuned field $\Omega \geq \Omega_0$. The potential of red detuned light, $\Omega \leq \Omega_0$, vice versa attracts the dots to the field antinodes. Use of both methods allows guiding and trapping of atomic matter waves.

References

- [1] H. Park, J. Park, A.K.L Lim, E.H. Anderson, A.P. Alivisatos, and P.L. McEuen, Nanomechanical oscillations in a single- C_{60} transistor, *Nature* 407, 57 (2000).
- [2] Pasupathy, A.N., et al., Vibration-assisted electron tunneling in C_{140} single-molecule transistors, *cond-mat/0311150*; J. Park , A. N. Pasupathy , J. I. Goldsmith , A. V. Soldatov , C. Chang , Y. Yaish , J. P. Sethna , H. D. Abruna , D. C. Ralph , P.L. McEuen, Wiring up single molecules, *Thin Solid Films* 438-439, 457-461 (2003).
- [3] Datta, S., *Electronic Transport in Mesoscopic Systems*, Cambridge studies in semiconductor physics and microelectronic engineering, ed. H. Ahmed, M. Pepper, and A. Broers. 1995, Cambridge, UK: Cambridge.
- [4] Park, J., et al., Coulomb blockade and the Kondo effect in single-atom transistors, *Nature* 417, 722-725, (2002).
- [5] L.H. Yu, D. Natelson, The Kondo effect in C_{60} single-molecule transistors, *Nano Letters* 4, 79 (2004).
- [6] D. Vion, A. Aassime, A. Cottet, P. Joyez, H. Pothier, C. Urbina, D. Esteve, M.H. Devoret, Manipulating the Quantum State of an Electrical Circuit *Science* 296, (2002), 886-889; E. Collin, G. Ithier, A. Aassime, P. Joyez, D. Vion, D. Esteve, NMR-like control of a quantum bit superconducting circuit, Submitted to *Phys. Rev. Lett.*
- [7] L.Y. Gorelik, A. Isacsson, M.V. Voinova, B. Kasemo, R.I. Shekhter, and M. Jonson, Shuttle Mechanism for Charge Transfer in Coulomb Blockade Nanostructures, *Phys. Rev. Lett.* 80, 4526 (1998).
- [8] C. Weiss, W. Zwerger, Accuracy of a mechanical single electron shuttle, *Europhys. Lett.* 47, 97 (1999).

- [9] M.T. Tuominen, R.V. Krotkov, and M.L. Breuer, Stepwise and Hysteretic Transport Behavior of an Electromechanical Charge Shuttle, *Physical Review Letters* 83, 3025-3028 (1999). R.V. Krotkov, M.T. Tuominen and M.L. Breuer, Charge Transport Experiments with Franklin's Bells, *Am. J. Phys.* 69, 50 (2001).
- [10] A.M.Dykhne, V.V. Zosimov, Tunnel Engine, *JETPh letters* 74, 366, (2001)
- [11] Gloria, B.Lubkin, Adiabatic quantum electron pump produce dc-current, *Physics Today* 52 (6), 19 (1999); M. Switkes, C. M. Marcus, K. Campman, A. C. Gossard, An Adiabatic Quantum Electron Pump, *Science* 283, 1905 (1999), B. Altshuler, L. Glazman, *ibid*, p. 1864.
- [12] S. Braig and K. Flensberg, Vibrational sidebands and dissipative tunneling in molecular transistors, *Phys. Rev. B* 68, 205324 (2003); K. Flensberg, *Phys. Rev. B* 68, 205323 (2003); S. Braig and K. Flensberg, Dissipative tunneling and orthogonality catastrophe in molecular transistors, *Phys. Rev. B* 70, 085317 (2004).
- [13] D. Boese, H. Schoeller, Influence of nano-mechanical properties on single electron tunneling: A vibrating Single-Electron Transistor, *Europhys. Lett.* 54, 668 (2001).
- [14] D. Fedorets, L.Y. Gorelik, R.I. Shekhter and M. Jonson, Vibrational instability due to coherent tunneling of electrons, *Europhys. Lett.* 58, 99 (2002).
- [15] S. A. Wolf et al, *Science* 294, 1488 (2001); *Semiconductor Spintronics and Quantum Computation*, edited by D. D. Awschalom et al., Berlin: Springer, 2002.
- [16] D.J.Thouless, Quantization of particle transport, *Phys.Rev.* B27, 6083 (1983).
- [17] A. Isacsson, T. Nord, Low frequency current noise of the single-electron shuttle, *cond-mat/0402228*.
- [18] Ya. M. Blanter, M. Buttiker, Shot Noise in Mesoscopic Conductors, *Phys. Rep.* 336, 1 (2000).
- [19] A. Kadigrobov, L. Y. Gorelik, R. I. Shekhter and M. Jonson, Resonant tunneling through Andreev levels, *cond-mat/9811212*.
- [20] F. Pistolesi, Full Counting Statistics of a charge shuttle, *Phys. Rev. B* 69, 245409 (2004).
- [21] The gap of $2\Omega = 10$ meV on the plots 2d and plot 3 in the work [1] still remains undocumented in details and unexplained in bulk of the theoretical papers.
- [22] L. Y. Gorelik, A. Isacsson, Y. M. Galperin, R. I. Shekhter and M. Jonson, *Nature* 411, 454 (2001).
- [23] A.P. Kazantsev, G.I.Surdutovich, Radiation of a Charged Particle Passing Close to a Metal Screen, *Sov. Phys. Dokl.* 7, 990 (1963).
- [24] L. V. Keldysh, *Zh. Eksp. Teor. Fiz.* 47, 1515 (1964); [*Sov. Phys. JETP* 20, 1018 (1965)].
- [25] A.O. Gogolin and A. Komnik, Multistable transport regimes and conformational changes in molecular quantum dots, *cond-mat/0207513*.
- [26] N. S. Wingreen and Y. Meir, *Phys. Rev. B* 49, 11040 (1994).
- [27] D. Mozyrsky and I. Martin, Measurement induced quantum-classical transition, *Phys. Rev. Lett.* 89, 018301 (2002).
- [28] V.M.Akulin, *Dynamics of Complex Quantum systems*, Chapter 4, Two band systems, Springer, 2004.
- [29] L. D. Landau and E. M. Lifshitz, *Quantum mechanics: non-relativistic theory*, New York: Pergamon Press, 1977.
- [30] Ovchinnikov, Shul'ga, and Balykin, *J. Phys. B: At. Mol. Opt. Phys.* 24, 3173 (1991)
- [31] A.Bezryadin, C.Dekker, and G.Schmid, Electrostatic trapping of single conducting nanoparticles between nanoelectrodes, *Appl. Phys. Lett.* 71, 1273-1275 (1997).
- [32] Y.Lin, I.Teper, C.Chin, V.Vuletic, Impact of Casimir-Polder potential and Johnson Noise on Bose-Einstein Condensate Stability Near Surfaces, *Phys. Rev. Lett.*, 92, 050404 (2004).

- [33] M. Hammes, D. Rychtarik, B. Engeser, H.-C. Nagerl, and R. Grimm, Evanescent-wave trapping and evaporative cooling of an atomic gas near two-dimensionality, physics/0208065.
- [34] A. Ashkin, Acceleration and Trapping of Particles by Radiation Pressure, *Phys. Rev. Lett.* 24, 156 (1970).
- [35] A. P. Kazantsev, *Zh. Eksp. Teor. Fiz.* 66, 1599 (1974) (*Sov. Phys. JETP* 39, 784 (1974)); A. P. Kazantsev, G.I. Surdutovich, and V.P. Yakovlev, *The mechanical Action of Light on Atoms*, Singapore: World Sci., 1990.
- [36] P. Kruger, X. Luo, M. W. Klein, K. Brugger, A. Haase, S. Wildermuth, S. Groth, I. Bar-Joseph, R. Folman, and J. Schmiedmayer, Trapping and Manipulating Neutral Atoms with Electrostatic Fields, *Phys. Rev. Lett.* 91, 233201 (2003).
- [37] D.M. Harber, J.M. McGuirk, J.M. Obrecht, and E.A. Cornell, Thermally Induced Losses in Ultra-Cold Atoms Magnetically Trapped Near Room-Temperature Surfaces *J. Low Temp. Phys.* 133, 229 (2003); J.M. McGuirk, D.M. Harber, J.M. Obrecht, E.A. Cornell, Alkali adsorbate polarization on conducting and insulating surfaces probed with Bose-Einstein condensates, cond-mat/0403254.
- [38] R. Dall, M. Hoogerland, K. Baldwin, J. Buckman, Hollow fibre guides for metastable helium atoms, *C. R. Acad. Sci. Paris* 2, (S. IV), 595-603 (2001).
- [39] S.N. Atutov, R. Calabrese, V. Guidi, B. Mai, A.G. Rudavets, E. Scansani, L. Tomassetti, V. Biancalana, A. Burchianti, C. Marinelli, E. Mariotti, L. Moi, S. Veronesi, Fast and efficient loading of a Rb magneto-optical trap using light-induced atomic desorption; *Phys. Rev. A* 67, 053401 (2003).
- [40] J. Chen, J.G. Story, J.J. Tollett, and R.G. Hulet, Adiabatic Cooling of Atoms by an Intense Blue-Detuned Standing Wave, *Physical Review Letters*, 69, 1344-1347 (1992).
- [41] L. Khaykovich, N. Davidson, Adiabatic focusing of cold atoms in a blue-detuned laser standing wave, *Appl. Phys. B*, 70, 683 (2000).
- [42] P. W. Anderson, *Phys. Rev. Lett.* 18, 1049 (1967).
- [43] I.O. Kulik and R.I. Shekhter, *Sov. Phys. JETP* 41, 308 (1975).
- [44] D.V. Averin and K.K. Likharev, in *Mesoscopic Phenomena in Solids*, edited by B.L. Altshuler, P. A. Lee, and R.A. Webb, Amsterdam: Elsevier, 173, 1991.
- [45] M. Abramowitz and I.A. Stegun, *Handbook of Mathematical Functions with Formulas, Graphs, and Mathematical Tables*, New York: Dover, 1972.
- [46] F. Dalfovo, S. Giorgini, L.P. Pitaevskii, S. Stringari, Theory of Bose-Einstein condensation in trapped gases, *Rev. Mod. Phys.* 71, 463-512 (1999).
- [47] S. Flügge, *Practical quantum mechanics*, Vol. 2, Cold electron emission, Springer-Verlag, 1971.